ELSEVIER

Ab initio potential energy surface, electric-dipole moment, polarizability tensor, and theoretical rovibrational spectra in the electronic ground state of $^{14}NH_3^+$

Sergei N. Yurchenko [a], Walter Thiel [b], Miguel Carvajal [c], Per Jensen [d,*]

[a] *Technische Universität Dresden, Institut für Physikalische Chemie und Elektrochemie, D-01062 Dresden, Germany*
[b] *Max-Planck-Institut für Kohlenforschung, Kaiser-Wilhelm-Platz 1, D-45470 Mülheim an der Ruhr, Germany*
[c] *Departamento de Fisica Aplicada, Facultad de Ciencias Experimentales, Avenida de las Fuerzas Armadas s/n, Universidad de Huelva, E-21071 Huelva, Spain*
[d] *Theoretische Chemie, Bergische Universität, D-42097 Wuppertal, Germany*

Abstract

We report the calculation of a six-dimensional CCSD(T)/aug-cc-pVQZ potential energy surface for the electronic ground state of NH_3^+ together with the corresponding CCSD(T)/aug-cc-pVTZ dipole moment and polarizability surface of $^{14}NH_3^+$. These electronic properties have been computed on a large grid of molecular geometries. A number of newly calculated band centers are presented along with the associated electric-dipole transition moments. We further report the first calculation of vibrational matrix elements of the polarizability tensor components for $^{14}NH_3^+$; these matrix elements determine the intensities of Raman transitions. In addition, the rovibrational absorption spectra of the v_2, v_3, v_4, $2v_2 - v_2$, and $v_2 + v_3 - v_2$ bands have been simulated.
© 2008 Elsevier B.V. All rights reserved.

1. Introduction

Thus far, there have been only few experimental, high-resolution spectroscopic studies of the ammonia cation NH_3^+. The experimental observations are limited to the infrared absorption bands v_3, v_2, and $v_2 \rightarrow 2v_2$, $v_2 \rightarrow v_2 + v_3$ [1–3]. At low resolution, the $^{14}NH_3^+$ ion has been studied by photoelectron and photoionization spectroscopy [4–15]. Further, the infrared spectrum of NH_3^+, trapped in a solid neon matrix, has been recorded [16]. To the best of our knowledge, no observation of the NH_3^+ Raman spectrum has been reported.

Theoretical studies of NH_3^+ are more abundant: a number of *ab initio* calculations have been done [17–25] to provide theoretical information and encourage experimental work. Considering only the variation of the two vibrational coordinates that describe the ion as having structures of C_{3v} geometrical symmetry (see for example, Ref. [26,27]), Botschwina [18–20] obtained a two-dimensional *ab initio* potential energy surface (PES) and the corresponding electric-dipole moment surface (DMS) with the coupled electron-pair approximation (CEPA) method [28]. With this *ab initio* information, he predicted many vibrational term values and relative infrared intensities [18–20] with an accuracy equaling that of present-day calculations. Špirko and Kraemer [21,22] calculated full-dimensional *ab initio* PESs at different levels of theory and a corresponding DMS was reported by Pracna et al. [23]. These authors used their DMS, together with a PES from Špirko

* Corresponding author. Tel.: +49 202 439 2468; fax: +49 202 439 2509.
E-mail address: jensen@uni-wuppertal.de (P. Jensen).

and Kraemer [21,22], for computing rovibrational energy levels and line strengths. In that work, special attention was paid to the symmetric out-of-plane bending mode (which turns into the "umbrella-flipping" inversion mode in NH_3). More recently, Viel et al. [25] have calculated the PES of NH_3^+ at the MR-CI level of theory with the purpose of studying the photoelectron spectrum of NH_3, taking into account the Jahn–Teller effect.

We report here the theoretical computation of spectral data (band centers and vibrational transition moments together with rovibrational transition wavenumbers and intensities) for electric dipole and Raman spectra of NH_3^+. These data are obtained from an *ab initio* PES with accompanying DMS and polarizability surface also calculated as part of the present work. Relative to previously published theoretical results [19–21,23] for NH_3^+, we have achieved a noticeable improvement in the reproduction of the extant experimental data. Our *ab initio* electronic-property surfaces are more accurate than those previously available and therefore more useful for the prediction of spectroscopic properties, especially for transitions involving highly excited states. We have generated, for the first time, the six-dimensional *ab initio* polarizability surface for NH_3^+.

In order to generate (ro)vibrational energies and intensities for the electric dipole and Raman spectra of NH_3^+, we solve the nuclear-motion Schrödinger equation variationally. In these calculations, we take into account all internal, nuclear degrees of freedom (i.e., all vibrational modes and the rotation). The theoretical procedure has been explained in Refs. [29,30] and applied to a number of pyramidal molecules: ammonia NH_3 [31,32], phosphine PH_3 [33–35] and, most recently, bismutine BiH_3 and stibine SbH_3 [36].

The NH_3^+ ion is planar at equilibrium with D_{3h} geometrical symmetry; its molecular symmetry (MS) group is $D_{3h}(M)$ [26,27], which is isomorphic to the point group D_{3h}. The irreducible representations of $D_{3h}(M)$ and D_{3h} are given in Table A-10 of Ref. [26]. The $D_{3h}(M)$ selection rules for vibrational transitions [26,27] are such that some of the fundamental vibrational transitions are forbidden in absorption and emission. This motivated us to supplement the information on such 'inactive' IR bands with information on the corresponding Raman transitions which satisfy other selection rules [26,27] so that they are not forbidden.

An important motivation for the present work is astrophysical: ammonia is found in comets, interstellar space, and planetary atmospheres [37–39]. Spectroscopic studies of NH_3 and related molecules lead to new understanding of these environments. For example, the nascent *ortho*-to-*para* ratio (OPR) for NH_3 in a comet can be interpreted to give the temperature of formation of the NH_3 species, and hence the temperature of formation of the comet; the temperature of formation of the comet indicates the distance from the solar nebula at which the comet was formed. The NH_3 OPR can be determined by analysis of the emission spectrum of NH_2 which derives from the pho-todissociation of NH_3 [40–42]. Interstellar microwave transitions have already been observed for NH_3 [37]. In addition nitrogen-containing, tetra-atomic ions such as $HCNH^+$ [43] have been detected in interstellar space, and so NH_3^+ appears a probable candidate for interstellar detection.

The paper is structured as follows. Section 2 discusses the *ab initio* PES and Section 3 is concerned with the DMS and the polarizability surface. In Section 4, we describe the computed vibrational bands, the electric-dipole transition moments, the polarizability tensor matrix elements and the intensity simulations of rovibrational absorption spectra. Finally, we present conclusions in Section 5.

2. The *ab initio* potential energy surface

The *ab initio* PES of NH_3^+ has been computed with the MOLPRO2002 [44,45] package at the UCCSD(T)/aug-cc-pVQZ level of theory (i.e., unrestricted coupled cluster theory with all single and double substitutions [46] and a perturbative treatment of connected triple excitations [47,48] with the augmented correlation-consistent quadruple-zeta basis [49,50]). Core-valence correlation effects were included at each point by adding the energy difference between all-electron and frozen-core UCCSD(T) calculations with the aug-cc-pCVTZ basis [51]. Throughout the paper this PES, and the level of theory at which it is calculated, will be referred to as AQZ. Following our previous work on XY_3 molecules [29], we represent the PES by an expansion (PES type A in Ref. [29])

$$
\begin{aligned}
V(\xi_1, \xi_2, \xi_3, \xi_{4a}, \xi_{4b}; \sin\bar{\rho}) = V_e + V_0(\sin\bar{\rho}) \\
+ \sum_j F_j(\sin\bar{\rho})\xi_j \\
+ \sum_{j\leqslant k} F_{jk}(\sin\bar{\rho})\xi_j\xi_k \\
+ \sum_{j\leqslant k\leqslant l} F_{jkl}(\sin\bar{\rho})\xi_j\xi_k\xi_l \\
+ \sum_{j\leqslant k\leqslant l\leqslant m} F_{jklm}(\sin\bar{\rho})\xi_j\xi_k\xi_l\xi_m
\end{aligned}
\tag{1}
$$

in terms of the variables

$$
\xi_i = 1 - \exp(-a(r_i - r_e)), \quad i = 1, 2, 3,
\tag{2}
$$

which describe the stretching motion,

$$
\xi_{4a} = \frac{1}{\sqrt{6}}(2\alpha_1 - \alpha_2 - \alpha_3),
\tag{3}
$$

$$
\xi_{4b} = \frac{1}{\sqrt{2}}(\alpha_2 - \alpha_3),
\tag{4}
$$

which describe the 'deformation' bending, and

$$
\sin\bar{\rho} = \frac{2}{\sqrt{3}}\sin[(\alpha_1 + \alpha_2 + \alpha_3)/6]
\tag{5}
$$

which describes the out-of-plane bending motion. In Eqs. (2)–(5), r_i is the instantaneous value of the internuclear distance N–H_i, $i = 1, 2, 3$, and the H–N–H bond angle α_i is 'opposite' to the r_i bond. We truncate the expansion in Eq. (1) after the fourth-order terms.

The pure out-of-plane-bending potential energy function in Eq. (1) is taken to be

$$V_0(\sin \bar{\rho}) = \sum_{s=1}^{4} f_0^{(s)} (\sin \rho_e - \sin \bar{\rho})^s, \tag{6}$$

and the functions $F_{jk\ldots}(\sin \bar{\rho})$ are defined as

$$F_{jk\ldots}(\sin \bar{\rho}) = \sum_{s=0}^{N} f_{jk\ldots}^{(s)} (\sin \rho_e - \sin \bar{\rho})^s, \tag{7}$$

where $\sin \rho_e = 1$ is the equilibrium value of $\sin \bar{\rho}$ and the quantities $f_0^{(s)}$ and $f_{jk\ldots}^{(s)}$ in Eqs. (6) and (7) are expansion coefficients. The summation limits in Eq. (7) are $N = 3$ for $F_j(\sin \bar{\rho})$, $N = 2$ for $F_{jk}(\sin \bar{\rho})$, $N = 1$ for $F_{jkl}(\sin \bar{\rho})$, $N = 0$ for $F_{jklm}(\sin \bar{\rho})$. In total there are 49 symmetrically unique potential parameters $f_{jk\ldots}^{(s)}$.

The Morse parameter a is fixed to the value 2.13 Å^{-1}. The 49 parameters $f_{jk\ldots}^{(s)}$ are obtained through fitting to 1251 *ab initio* energies computed for a set of geometries covering the range $0.9 \text{ Å} \leqslant r_1 \leqslant r_2 \leqslant r_3 \leqslant 1.2 \text{ Å}$ and $90° \leqslant \alpha_1, \alpha_2, \alpha_3 \leqslant 120°$. The root-mean-square (rms) devia-

tion of the fitting is 0.25 cm^{-1}. The optimized potential-energy parameter values are listed in Table 1.

3. The molecular dipole moment and the polarizability tensor

The *ab initio* dipole moment (DM) and polarizability tensor (PT) values employed in the present work were computed with the MOLPRO2002 [44,45] package at the RCCSD(T)/aug-cc-pVTZ level of theory [46–50] in the frozen-core approximation. Throughout the paper the DM and PT surfaces, together with the level of theory at which they are calculated, will be referred to as ATZfc. Dipole moment and polarizability tensor values were computed in a numerical finite-difference procedure with an added external dipole field of 0.001 a.u.

The *ab initio* dipole moment components were calculated at 2281 geometries covering the same geometry range that was used for the PES. The polarizability tensor has six independent components, and in order to describe them accurately, it was necessary to compute them on an extended grid of 2661 points. Following Refs. [30,32,52, 53] we use the molecular bond (MB) representation to describe the r_i and α_j dependence of the electronically averaged dipole moment vector [26,30] $\bar{\mu}$ for NH_3^+. In the MB representation, this vector is given by

$$\bar{\mu} = \bar{\mu}_1^{\text{Bond}} \mathbf{e}_1 + \bar{\mu}_2^{\text{Bond}} \mathbf{e}_2 + \bar{\mu}_3^{\text{Bond}} \mathbf{e}_3 \tag{8}$$

where the three functions $\bar{\mu}_i^{\text{Bond}}$, $i = 1, 2, 3$, depend on the vibrational coordinates, and $\mathbf{e}_i$ is the unit vector along the N–H_i bond,

$$\mathbf{e}_i = \frac{\mathbf{r}_i - \mathbf{r}_4}{|\mathbf{r}_i - \mathbf{r}_4|} \tag{9}$$

with $\mathbf{r}_i$ as the position vector of nucleus i (the protons are labeled 1, 2, 3, and the nitrogen nucleus is labeled 4). The representation of $\bar{\mu}$ in Eq. (8) is 'body-fixed' in the sense that it relates the dipole moment vector directly to the instantaneous positions of the nuclei (i.e., to the vectors $\mathbf{r}_i$) [30].

Following Refs. [30,32], we express the three functions $\bar{\mu}_i^{\text{Bond}}$, $i = 1, 2, 3$, in terms of the projections of $\bar{\mu}$ onto the N–H bonds

$$\bar{\mu}_i^{\text{Bond}} = \sum_{j=1}^{3} (\mathbf{A}^{-1})_{ij} (\bar{\mu} \cdot \mathbf{e}_j) \tag{10}$$

where $(\mathbf{A}^{-1})_{ij}$ is an element of the non-orthogonal 3×3 matrix $\mathbf{A}^{-1}$ obtained as the inverse[1] of

Table 1
Ab initio potential energy parameters (in cm^{-1} unless otherwise indicated) for the electronic ground state of NH_3^+

Parameter	Value	Parameter	Value
r_e (Å)	1.0207036(11)[a]	f_{114}^1	−9342(214)
a (Å^{-1})	2.13[b]	f_{123}^0	−425.9(77)
f_0^1	57,472.2(64)	f_{123}^1	2719(318)
f_0^2	364,126(337)	f_{124}^0	1033.1(79)
f_0^3	−853,100(6027)	f_{124}^1	7343(196)
f_0^4	2,042,989(34772)	f_{144}^0	−1326(17)
f_1^1	−19,613(15)	f_{144}^1	−7881(314)
f_1^2	2021(537)	f_{155}^0	−2973(19)
f_1^3	−59,330(4946)	f_{155}^1	−6538(351)
f_{11}^0	37,674.58(92)	f_{455}^0	5339(25)
f_{11}^1	−8710(35)	f_{455}^1	13,017(376)
f_{11}^2	−26,408(627)	f_{1111}^0	3693.5(80)
f_{12}^0	−130.3(12)	f_{1112}^0	−99.8(79)
f_{12}^1	5277(48)	f_{1114}^0	−391(15)
f_{12}^2	13,150(851)	f_{1122}^0	−89(11)
f_{14}^0	−1315.2(54)	f_{1123}^0	−242(19)
f_{14}^1	−18,267(250)	f_{1124}^0	340(17)
f_{14}^2	3788(2425)	f_{1125}^0	618(25)
f_{44}^0	11,461.3(42)	f_{1144}^0	−937(25)
f_{44}^1	54,250(165)	f_{1155}^0	−2514(34)
f_{44}^2	−112,973(1583)	f_{1244}^0	504(18)
f_{111}^0	491.2(19)	f_{1255}^0	1570(27)
f_{111}^1	−4170(82)	f_{1444}^0	−611(36)
f_{112}^0	24.4(20)	f_{1455}^0	−856(55)
f_{112}^1	1392(92)	f_{4444}^0	−155(10)
f_{114}^0	−725.7(97)		

[a] Quantities in parentheses are standard errors in units of the last digit given.
[b] Held fixed in the least-squares fitting.

---

[1] We have already discussed in Refs. [30,32] that at planar configurations where $\alpha_1 + \alpha_2 + \alpha_3 = 2\pi$, the determinant $|\mathbf{A}| = 0$ and $\mathbf{A}^{-1}$ does not exist. This is because $\mathbf{e}_1$, $\mathbf{e}_2$, and $\mathbf{e}_3$ are linearly dependent and there are infinitely many possible values of $(\bar{\mu}_1^{\text{Bond}}, \bar{\mu}_2^{\text{Bond}}, \bar{\mu}_3^{\text{Bond}})$. In this case we set $\bar{\mu}_3^{\text{Bond}} = 0$ in Eq. (8) and express $\bar{\mu}$ in terms of $\mathbf{e}_1$ and $\mathbf{e}_2$ only.

Table 2
ATZfc electric-dipole moment parameters[a] in the MB representation for the electronic ground state of $^{14}NH_3^+$ (see Eq. (15))

Parameter	Value	Parameter	Value	Parameter	Value
b (Å^{-1})	1.15	$\mu_{266}^{(0)}$ (D Å^{-1})	2.878810	$\mu_{1666}^{(0)}$ (D Å^{-1})	0.558748
$\mu_{1}^{(0)}$ (D Å^{-1})	−6.843604	$\mu_{333}^{(0)}$ (D Å^{-3})	−6.361674	$\mu_{2222}^{(0)}$ (D Å^{-4})	19.646100
$\mu_{3}^{(0)}$ (D Å^{-1})	3.434735	$\mu_{334}^{(0)}$ (D Å^{-2})	2.186843	$\mu_{2224}^{(0)}$ (D Å^{-3})	−3.219553
$\mu_{4}^{(0)}$ (D)	1.012222	$\mu_{344}^{(0)}$ (D Å^{-1})	−0.200454	$\mu_{2225}^{(0)}$ (D Å^{-3})	4.237734
$\mu_{5}^{(0)}$ (D)	2.069054	$\mu_{444}^{(0)}$ (D)	0.130048	$\mu_{2244}^{(0)}$ (D Å^{-2})	0.288955
$\mu_{11}^{(0)}$ (D Å^{-2})	4.835573	$\mu_{445}^{(0)}$ (D)	0.073544	$\mu_{2245}^{(0)}$ (D Å^{-2})	−0.811717
$\mu_{13}^{(0)}$ (D Å^{-2})	−3.175562	$\mu_{456}^{(0)}$ (D)	0.632632	$\mu_{2246}^{(0)}$ (D Å^{-2})	−0.516277
$\mu_{14}^{(0)}$ (D Å^{-1})	−4.264478	$\mu_{466}^{(0)}$ (D)	−0.082600	$\mu_{2255}^{(0)}$ (D Å^{-2})	−0.399009
$\mu_{16}^{(0)}$ (D Å^{-1})	5.651595	$\mu_{555}^{(0)}$ (D)	0.060544	$\mu_{2256}^{(0)}$ (D Å^{-2})	2.206634
$\mu_{23}^{(0)}$ (D Å^{-2})	6.823521	$\mu_{556}^{(0)}$ (D)	−0.132632	$\mu_{2266}^{(0)}$ (D Å^{-2})	−1.555935
$\mu_{33}^{(0)}$ (D Å^{-2})	−2.808766	$\mu_{1111}^{(0)}$ (D Å^{-4})	−35.944039	$\mu_{2333}^{(0)}$ (D Å^{-4})	9.500434
$\mu_{34}^{(0)}$ (D Å^{-1})	−0.843761	$\mu_{1112}^{(0)}$ (D Å^{-4})	−10.497074	$\mu_{2334}^{(0)}$ (D Å^{-3})	2.655695
$\mu_{35}^{(0)}$ (D Å^{-1})	−12.640348	$\mu_{1114}^{(0)}$ (D Å^{-3})	−9.457721	$\mu_{2335}^{(0)}$ (D Å^{-3})	1.774231
$\mu_{36}^{(0)}$ (D Å^{-1})	2.399561	$\mu_{1115}^{(0)}$ (D Å^{-3})	8.802863	$\mu_{2336}^{(0)}$ (D Å^{-3})	−0.523673
$\mu_{46}^{(0)}$ (D)	−0.117599	$\mu_{1122}^{(0)}$ (D Å^{-4})	2.630873	$\mu_{2344}^{(0)}$ (D Å^{-2})	0.648306
$\mu_{55}^{(0)}$ (D)	−0.504553	$\mu_{1124}^{(0)}$ (D Å^{-3})	−3.312608	$\mu_{2345}^{(0)}$ (D Å^{-2})	1.090952
$\mu_{56}^{(0)}$ (D)	0.388056	$\mu_{1126}^{(0)}$ (D Å^{-3})	0.401930	$\mu_{2356}^{(0)}$ (D Å^{-2})	−0.573295
$\mu_{111}^{(0)}$ (D Å^{-3})	13.779441	$\mu_{1136}^{(0)}$ (D Å^{-3})	3.997013	$\mu_{2366}^{(0)}$ (D Å^{-2})	−1.475248
$\mu_{112}^{(0)}$ (D Å^{-3})	10.049993	$\mu_{1144}^{(0)}$ (D Å^{-2})	0.938232	$\mu_{2444}^{(0)}$ (D Å^{-1})	−0.087380
$\mu_{114}^{(0)}$ (D Å^{-2})	9.691422	$\mu_{1146}^{(0)}$ (D Å^{-2})	2.075752	$\mu_{2445}^{(0)}$ (D Å^{-1})	0.655178
$\mu_{115}^{(0)}$ (D Å^{-2})	−8.706157	$\mu_{1155}^{(0)}$ (D Å^{-2})	−0.593303	$\mu_{2455}^{(0)}$ (D Å^{-1})	−0.013374
$\mu_{123}^{(0)}$ (D Å^{-3})	−2.220674	$\mu_{1156}^{(0)}$ (D Å^{-2})	−2.217717	$\mu_{2456}^{(0)}$ (D Å^{-1})	−1.782524
$\mu_{124}^{(0)}$ (D Å^{-2})	2.341861	$\mu_{1222}^{(0)}$ (D Å^{-4})	−6.570507	$\mu_{2466}^{(0)}$ (D Å^{-1})	0.858035
$\mu_{135}^{(0)}$ (D Å^{-2})	−1.907079	$\mu_{1225}^{(0)}$ (D Å^{-3})	2.328468	$\mu_{3335}^{(0)}$ (D Å^{-3})	−31.175997
$\mu_{136}^{(0)}$ (D Å^{-2})	−4.551584	$\mu_{1233}^{(0)}$ (D Å^{-4})	2.443607	$\mu_{3445}^{(0)}$ (D Å^{-1})	−0.229146
$\mu_{144}^{(0)}$ (D Å^{-1})	−0.890388	$\mu_{1234}^{(0)}$ (D Å^{-3})	−1.174183	$\mu_{3555}^{(0)}$ (D Å^{-1})	−0.378778
$\mu_{146}^{(0)}$ (D Å^{-1})	−1.834530	$\mu_{1235}^{(0)}$ (D Å^{-3})	−1.605869	$\mu_{3556}^{(0)}$ (D Å^{-1})	−0.448908
$\mu_{155}^{(0)}$ (D Å^{-1})	−1.328220	$\mu_{1245}^{(0)}$ (D Å^{-2})	0.584696	$\mu_{3566}^{(0)}$ (D Å^{-1})	−0.102296
$\mu_{156}^{(0)}$ (D Å^{-1})	1.298989	$\mu_{1246}^{(0)}$ (D Å^{-2})	−0.394594	$\mu_{3666}^{(0)}$ (D Å^{-1})	0.071158
$\mu_{223}^{(0)}$ (D Å^{-3})	−8.850826	$\mu_{1256}^{(0)}$ (D Å^{-2})	−0.386002	$\mu_{4444}^{(0)}$ (D)	−0.049562
$\mu_{225}^{(0)}$ (D Å^{-2})	−3.858900	$\mu_{1334}^{(0)}$ (D Å^{-3})	0.555470	$\mu_{4445}^{(0)}$ (D)	−0.027221
$\mu_{226}^{(0)}$ (D Å^{-2})	25.883368	$\mu_{1335}^{(0)}$ (D Å^{-3})	2.405382	$\mu_{4456}^{(0)}$ (D)	−0.368059
$\mu_{234}^{(0)}$ (D Å^{-2})	−4.044328	$\mu_{1355}^{(0)}$ (D Å^{-2})	1.044514	$\mu_{4466}^{(0)}$ (D)	0.280112
$\mu_{235}^{(0)}$ (D Å^{-2})	−0.669207	$\mu_{1366}^{(0)}$ (D Å^{-2})	−0.165703	$\mu_{4555}^{(0)}$ (D)	−0.080231
$\mu_{245}^{(0)}$ (D Å^{-1})	−0.523503	$\mu_{1445}^{(0)}$ (D Å^{-1})	−0.084613	$\mu_{4556}^{(0)}$ (D)	−0.532429
$\mu_{246}^{(0)}$ (D Å^{-1})	1.263005	$\mu_{1456}^{(0)}$ (D Å^{-1})	1.941205	$\mu_{5566}^{(0)}$ (D)	0.477874
$\mu_{255}^{(0)}$ (D Å^{-1})	0.873503	$\mu_{1466}^{(0)}$ (D Å^{-1})	−0.591163	$\mu_{5666}^{(0)}$ (D)	0.093791
$\mu_{256}^{(0)}$ (D Å^{-1})	−1.294535	$\mu_{1566}^{(0)}$ (D Å^{-1})	1.023531	$\mu_{6666}^{(0)}$ (D)	0.020529

[a] The parameter values in the table define, in conjunction with Eqs. (10)–(18), a dipole moment vector expressed in an axis system with origin at the center of mass for $^{14}NH_3^+$.

$$\mathbf{A} = \begin{pmatrix} 1 & \cos\alpha_3 & \cos\alpha_2 \\ \cos\alpha_3 & 1 & \cos\alpha_1 \\ \cos\alpha_2 & \cos\alpha_1 & 1 \end{pmatrix}. \quad (11)$$

All three projections are given in terms of a single function $\bar{\mu}_0(r_1, r_2, r_3, \alpha_1, \alpha_2, \alpha_3)$ [30]:

$$\bar{\boldsymbol{\mu}} \cdot \mathbf{e}_1 = \bar{\mu}_0(r_1, r_2, r_3, \alpha_1, \alpha_2, \alpha_3) = \bar{\mu}_0(r_1, r_3, r_2, \alpha_1, \alpha_3, \alpha_2), \quad (12)$$

$$\bar{\boldsymbol{\mu}} \cdot \mathbf{e}_2 = \bar{\mu}_0(r_2, r_3, r_1, \alpha_2, \alpha_3, \alpha_1) = \bar{\mu}_0(r_2, r_1, r_3, \alpha_2, \alpha_1, \alpha_3), \quad (13)$$

$$\bar{\boldsymbol{\mu}} \cdot \mathbf{e}_3 = \bar{\mu}_0(r_3, r_1, r_2, \alpha_3, \alpha_1, \alpha_2) = \bar{\mu}_0(r_3, r_2, r_1, \alpha_3, \alpha_2, \alpha_1). \quad (14)$$

This function is expressed as an expansion

$$\bar{\mu}_0 = \sum_k \mu_k^{(0)} \zeta_k + \sum_{k,l} \mu_{kl}^{(0)} \zeta_k \zeta_l + \sum_{k,l,m} \mu_{klm}^{(0)} \zeta_k \zeta_l \zeta_m + \sum_{k,l,m,n} \mu_{klmn}^{(0)} \zeta_k \zeta_l \zeta_m \zeta_n \quad (15)$$

in the variables

Table 3
ATZfc polarizability tensor parameters[a] $\alpha_{ijk\ldots}^{(0)}$ in the MB representation for the electronic ground state of $^{14}NH_3^+$ (see Eq. (30) with $c = \alpha$)

Parameter	Value	Parameter	Value	Parameter	Value
b (Å^{-1})	0	$\alpha_{256}^{(0)}$ (Å^2)	−0.989074	$\alpha_{1466}^{(0)}$ (Å^2)	−0.062063
$\alpha_{1}^{(0)}$ (Å^2)	0.493404	$\alpha_{266}^{(0)}$ (Å^2)	1.952151	$\alpha_{1566}^{(0)}$ (Å^2)	−0.189215
$\alpha_{3}^{(0)}$ (Å^2)	−0.465832	$\alpha_{333}^{(0)}$	−0.460974	$\alpha_{2222}^{(0)}$ (Å^{-1})	0.076761
$\alpha_{4}^{(0)}$ (Å^3)	0.445852	$\alpha_{334}^{(0)}$ (Å)	−0.055144	$\alpha_{2224}^{(0)}$	−0.046087
$\alpha_{5}^{(0)}$ (Å^3)	−0.284352	$\alpha_{344}^{(0)}$ (Å^2)	0.024214	$\alpha_{2244}^{(0)}$ (Å)	−0.028324
$\alpha_{11}^{(0)}$ (Å)	−1.189665	$\alpha_{444}^{(0)}$ (Å^3)	−0.044236	$\alpha_{2245}^{(0)}$ (Å)	0.021640
$\alpha_{13}^{(0)}$ (Å)	−0.169320	$\alpha_{445}^{(0)}$ (Å^3)	0.137282	$\alpha_{2246}^{(0)}$ (Å)	−0.072515
$\alpha_{14}^{(0)}$ (Å^2)	−1.447197	$\alpha_{456}^{(0)}$ (Å^3)	−0.700875	$\alpha_{2255}^{(0)}$ (Å)	0.019044
$\alpha_{16}^{(0)}$ (Å^2)	0.560079	$\alpha_{466}^{(0)}$ (Å^3)	0.097452	$\alpha_{2256}^{(0)}$ (Å)	0.116615
$\alpha_{23}^{(0)}$ (Å)	−0.312925	$\alpha_{555}^{(0)}$ (Å^3)	0.026306	$\alpha_{2266}^{(0)}$ (Å)	−1.323202
$\alpha_{33}^{(0)}$ (Å)	0.540775	$\alpha_{556}^{(0)}$ (Å^3)	0.137435	$\alpha_{2334}^{(0)}$	0.136829
$\alpha_{34}^{(0)}$ (Å^2)	0.050189	$\alpha_{1111}^{(0)}$ (Å^{-1})	−0.136197	$\alpha_{2335}^{(0)}$	0.054877
$\alpha_{35}^{(0)}$ (Å^2)	0.911449	$\alpha_{1112}^{(0)}$ (Å^{-1})	−0.194616	$\alpha_{2336}^{(0)}$	−0.201638
$\alpha_{36}^{(0)}$ (Å^2)	−0.311468	$\alpha_{1114}^{(0)}$	−0.476985	$\alpha_{2344}^{(0)}$ (Å)	0.063080
$\alpha_{46}^{(0)}$ (Å^3)	−0.267262	$\alpha_{1115}^{(0)}$	−0.105702	$\alpha_{2345}^{(0)}$ (Å)	−0.042955
$\alpha_{55}^{(0)}$ (Å^3)	−1.014634	$\alpha_{1122}^{(0)}$ (Å^{-1})	−0.182241	$\alpha_{2356}^{(0)}$ (Å)	0.772595
$\alpha_{56}^{(0)}$ (Å^3)	1.111683	$\alpha_{1124}^{(0)}$	−0.013455	$\alpha_{2366}^{(0)}$ (Å)	−0.061730
$\alpha_{111}^{(0)}$	0.496223	$\alpha_{1126}^{(0)}$	0.387104	$\alpha_{2445}^{(0)}$ (Å^2)	−0.055619
$\alpha_{112}^{(0)}$	0.397490	$\alpha_{1136}^{(0)}$	−0.046041	$\alpha_{2455}^{(0)}$ (Å^2)	0.030787
$\alpha_{114}^{(0)}$ (Å)	1.394169	$\alpha_{1144}^{(0)}$ (Å)	0.037216	$\alpha_{2456}^{(0)}$ (Å^2)	−0.061066
$\alpha_{115}^{(0)}$ (Å)	−0.132916	$\alpha_{1146}^{(0)}$ (Å)	−0.089148	$\alpha_{2466}^{(0)}$ (Å^2)	−0.105342
$\alpha_{123}^{(0)}$	0.251988	$\alpha_{1155}^{(0)}$ (Å)	−0.106994	$\alpha_{3335}^{(0)}$	0.243145
$\alpha_{124}^{(0)}$ (Å)	0.145328	$\alpha_{1156}^{(0)}$ (Å)	0.243709	$\alpha_{3445}^{(0)}$ (Å^2)	0.043989
$\alpha_{135}^{(0)}$ (Å)	−1.904524	$\alpha_{1222}^{(0)}$ (Å^{-1})	0.061230	$\alpha_{3555}^{(0)}$ (Å^2)	−0.085116
$\alpha_{136}^{(0)}$ (Å)	0.298890	$\alpha_{1225}^{(0)}$	−0.145562	$\alpha_{3556}^{(0)}$ (Å^2)	−0.015273
$\alpha_{144}^{(0)}$ (Å^2)	−0.060657	$\alpha_{1233}^{(0)}$ (Å^{-1})	−0.098227	$\alpha_{3566}^{(0)}$ (Å^2)	0.043723
$\alpha_{146}^{(0)}$ (Å^2)	0.401608	$\alpha_{1234}^{(0)}$	−0.129946	$\alpha_{3666}^{(0)}$ (Å^2)	−0.008463
$\alpha_{155}^{(0)}$ (Å^2)	0.335064	$\alpha_{1235}^{(0)}$	0.019214	$\alpha_{4444}^{(0)}$ (Å^3)	0.023417
$\alpha_{156}^{(0)}$ (Å^2)	−0.490512	$\alpha_{1245}^{(0)}$ (Å)	−0.291728	$\alpha_{4445}^{(0)}$ (Å^3)	0.016761
$\alpha_{223}^{(0)}$	0.117860	$\alpha_{1246}^{(0)}$ (Å)	0.256699	$\alpha_{4456}^{(0)}$ (Å^3)	0.196531
$\alpha_{225}^{(0)}$ (Å)	0.269858	$\alpha_{1256}^{(0)}$ (Å)	0.070449	$\alpha_{4466}^{(0)}$ (Å^3)	−0.037671
$\alpha_{226}^{(0)}$ (Å)	−0.530312	$\alpha_{1334}^{(0)}$	0.015997	$\alpha_{4555}^{(0)}$ (Å^3)	0.059061
$\alpha_{234}^{(0)}$ (Å)	−0.279805	$\alpha_{1335}^{(0)}$	0.967789	$\alpha_{4556}^{(0)}$ (Å^3)	0.169423
$\alpha_{235}^{(0)}$ (Å)	0.095014	$\alpha_{1355}^{(0)}$ (Å)	0.010522	$\alpha_{5566}^{(0)}$ (Å^3)	−0.201868
$\alpha_{245}^{(0)}$ (Å^2)	0.177348	$\alpha_{1366}^{(0)}$ (Å)	−0.037858	$\alpha_{5666}^{(0)}$ (Å^3)	−0.049009
$\alpha_{246}^{(0)}$ (Å^2)	0.047253	$\alpha_{1445}^{(0)}$ (Å^2)	−0.195151	$\alpha_{6666}^{(0)}$ (Å^3)	0.030824
$\alpha_{255}^{(0)}$ (Å^2)	0.058489	$\alpha_{1456}^{(0)}$ (Å^2)	0.652634		

[a] In the cgs unit system, the static polarizability tensor components have units of cm^3. We use here the related unit Å$^3 = 10^{-24}$ cm^3.

Table 4
ATZfc polarizability tensor parameters[a] $\gamma_{ijk\ldots}^{(0)}$ in the MB representation for the electronic ground state of $^{14}NH_3^+$ (see Eq. (30) with $c = \gamma$)

Parameter	Value	Parameter	Value	Parameter	Value
b (Å^{-1})	0	$\gamma_{256}^{(0)}$ (Å^2)	−0.581908	$\gamma_{1666}^{(0)}$ (Å^2)	−0.031633
$\gamma_{1}^{(0)}$ (Å^2)	0.571253	$\gamma_{266}^{(0)}$ (Å^2)	−0.014717	$\gamma_{2224}^{(0)}$	−0.790934
$\gamma_{3}^{(0)}$ (Å^2)	−0.158345	$\gamma_{334}^{(0)}$ (Å)	1.770157	$\gamma_{2225}^{(0)}$	0.149684
$\gamma_{4}^{(0)}$ (Å^3)	1.064409	$\gamma_{344}^{(0)}$ (Å^2)	−0.100991	$\gamma_{2244}^{(0)}$ (Å)	−0.312831
$\gamma_{5}^{(0)}$ (Å^3)	−0.671033	$\gamma_{444}^{(0)}$ (Å^3)	0.095695	$\gamma_{2245}^{(0)}$ (Å)	−0.091105
$\gamma_{11}^{(0)}$ (Å)	−0.971826	$\gamma_{445}^{(0)}$ (Å^3)	0.022256	$\gamma_{2246}^{(0)}$ (Å)	−0.350528
$\gamma_{13}^{(0)}$ (Å)	0.167939	$\gamma_{456}^{(0)}$ (Å^3)	−0.137319	$\gamma_{2255}^{(0)}$ (Å)	0.034223
$\gamma_{14}^{(0)}$ (Å^2)	−0.571641	$\gamma_{466}^{(0)}$ (Å^3)	−0.167322	$\gamma_{2266}^{(0)}$ (Å)	−0.027770
$\gamma_{16}^{(0)}$ (Å^2)	0.607798	$\gamma_{555}^{(0)}$ (Å^3)	−0.041107	$\gamma_{2333}^{(0)}$ (Å^{-1})	0.234003
$\gamma_{23}^{(0)}$ (Å)	0.646475	$\gamma_{556}^{(0)}$ (Å^3)	−0.040988	$\gamma_{2334}^{(0)}$	−0.222918
$\gamma_{33}^{(0)}$ (Å)	0.136753	$\gamma_{1111}^{(0)}$ (Å^{-1})	−0.194871	$\gamma_{2335}^{(0)}$	0.178192
$\gamma_{34}^{(0)}$ (Å^2)	−1.972865	$\gamma_{1114}^{(0)}$	0.010980	$\gamma_{2336}^{(0)}$	0.099244
$\gamma_{35}^{(0)}$ (Å^2)	−0.058342	$\gamma_{1115}^{(0)}$	0.154238	$\gamma_{2344}^{(0)}$ (Å)	0.708195
$\gamma_{36}^{(0)}$ (Å^2)	1.462181	$\gamma_{1122}^{(0)}$ (Å^{-1})	−0.074861	$\gamma_{2345}^{(0)}$ (Å)	−0.131913
$\gamma_{46}^{(0)}$ (Å^3)	0.308868	$\gamma_{1124}^{(0)}$	−0.055953	$\gamma_{2356}^{(0)}$ (Å)	0.410695
$\gamma_{55}^{(0)}$ (Å^3)	0.187358	$\gamma_{1126}^{(0)}$	0.055629	$\gamma_{2366}^{(0)}$ (Å)	0.100046
$\gamma_{56}^{(0)}$ (Å^3)	−0.172508	$\gamma_{1136}^{(0)}$	0.405061	$\gamma_{2444}^{(0)}$ (Å^2)	−0.033803
$\gamma_{111}^{(0)}$	0.699937	$\gamma_{1144}^{(0)}$ (Å)	−0.068093	$\gamma_{2445}^{(0)}$ (Å^2)	0.034601
$\gamma_{112}^{(0)}$	−0.043259	$\gamma_{1146}^{(0)}$ (Å)	0.079653	$\gamma_{2455}^{(0)}$ (Å^2)	0.009920
$\gamma_{115}^{(0)}$ (Å)	−0.309539	$\gamma_{1155}^{(0)}$ (Å)	0.043053	$\gamma_{2456}^{(0)}$ (Å^2)	0.134212
$\gamma_{123}^{(0)}$	−0.161635	$\gamma_{1156}^{(0)}$ (Å)	−1.476878	$\gamma_{2466}^{(0)}$ (Å^2)	0.101537
$\gamma_{124}^{(0)}$ (Å)	0.584183	$\gamma_{1222}^{(0)}$ (Å^{-1})	0.063065	$\gamma_{3335}^{(0)}$	−0.183962
$\gamma_{135}^{(0)}$ (Å)	−0.178955	$\gamma_{1225}^{(0)}$	0.240693	$\gamma_{3445}^{(0)}$ (Å^2)	0.079421
$\gamma_{136}^{(0)}$ (Å)	−0.973424	$\gamma_{1233}^{(0)}$ (Å^{-1})	0.064625	$\gamma_{3555}^{(0)}$ (Å^2)	0.006624
$\gamma_{144}^{(0)}$ (Å^2)	0.143030	$\gamma_{1234}^{(0)}$	−0.271015	$\gamma_{3556}^{(0)}$ (Å^2)	0.126310
$\gamma_{146}^{(0)}$ (Å^2)	−0.760431	$\gamma_{1245}^{(0)}$ (Å)	0.129446	$\gamma_{3566}^{(0)}$ (Å^2)	−0.014971
$\gamma_{155}^{(0)}$ (Å^2)	0.062305	$\gamma_{1246}^{(0)}$ (Å)	0.575131	$\gamma_{3666}^{(0)}$ (Å^2)	0.045119
$\gamma_{156}^{(0)}$ (Å^2)	2.070483	$\gamma_{1256}^{(0)}$ (Å)	0.077033	$\gamma_{4444}^{(0)}$ (Å^3)	−0.025655
$\gamma_{223}^{(0)}$	−0.396710	$\gamma_{1334}^{(0)}$	−0.268837	$\gamma_{4445}^{(0)}$ (Å^3)	−0.050596
$\gamma_{225}^{(0)}$ (Å)	−0.782040	$\gamma_{1335}^{(0)}$	−0.060920	$\gamma_{4456}^{(0)}$ (Å^3)	0.211031
$\gamma_{226}^{(0)}$ (Å)	0.550283	$\gamma_{1355}^{(0)}$ (Å)	−0.119683	$\gamma_{4466}^{(0)}$ (Å^3)	−0.163845
$\gamma_{234}^{(0)}$ (Å)	0.468093	$\gamma_{1366}^{(0)}$ (Å)	0.051170	$\gamma_{4555}^{(0)}$ (Å^3)	−0.022778
$\gamma_{235}^{(0)}$ (Å)	−0.577397	$\gamma_{1445}^{(0)}$ (Å^2)	−0.055251	$\gamma_{4556}^{(0)}$ (Å^3)	0.085410
$\gamma_{245}^{(0)}$ (Å^2)	0.113045	$\gamma_{1456}^{(0)}$ (Å^2)	−0.168697	$\gamma_{5566}^{(0)}$ (Å^3)	−0.028347
$\gamma_{246}^{(0)}$ (Å^2)	0.106509	$\gamma_{1466}^{(0)}$ (Å^2)	0.067165	$\gamma_{5666}^{(0)}$ (Å^3)	0.037276
$\gamma_{255}^{(0)}$ (Å^2)	−0.277997	$\gamma_{1566}^{(0)}$ (Å^2)	−0.112153	$\gamma_{6666}^{(0)}$ (Å^3)	0.002851

[a] In the cgs unit system, the static polarizability tensor components have units of cm^3. We use here the related unit Å$^3 = 10^{-24}$ cm^3.

$$\zeta_k = r_k \exp\left(-b^2 r_k^2\right), \quad k = 1, 2, 3, \tag{16}$$

$$\zeta_l = \cos(\alpha_{l-3}) - \cos\left(\frac{2\pi}{3}\right) = \frac{1}{2} + \cos(\alpha_{l-3}), \quad l = 4, 5, 6. \tag{17}$$

We include the factor $\exp(-b^2 r_k^2)$ in Eq. (16), with a suitably chosen value of the parameter b, in order to prevent the expansion from diverging at large r_k [32,53].

The expansion coefficients $\mu_{klm\ldots}^{(0)}$ in Eq. (15) obey the following permutation rules:

$$\mu_{k'l'm'\ldots}^{(0)} = \mu_{klm\ldots}^{(0)} \tag{18}$$

Table 5
ATZfc polarizability tensor parameters[a] $\delta^{(0)}_{ijk...}$ in the MB representation for the electronic ground state of $^{14}NH_3^+$ (see Eq. (30) with $c = \delta$)

Parameter	Value	Parameter	Value	Parameter	Value
b (Å^{-1})	0	$\delta^{(0)}_{333}$	0.491484	$\delta^{(0)}_{1236}$	0.229499
$\delta^{(0)}_{0}$ (Å^3)	−0.302838	$\delta^{(0)}_{356}$ (Å^2)	−0.171005	$\delta^{(0)}_{1245}$ (Å)	0.303504
$\delta^{(0)}_{4}$ (Å^3)	0.057101	$\delta^{(0)}_{366}$ (Å^2)	−0.164452	$\delta^{(0)}_{1255}$ (Å)	−0.017150
$\delta^{(0)}_{11}$ (Å)	−0.638935	$\delta^{(0)}_{456}$ (Å^3)	−0.250350	$\delta^{(0)}_{1256}$ (Å)	0.189312
$\delta^{(0)}_{13}$ (Å)	0.368525	$\delta^{(0)}_{556}$ (Å^3)	−0.010198	$\delta^{(0)}_{1266}$ (Å)	0.208419
$\delta^{(0)}_{14}$ (Å^2)	−0.346979	$\delta^{(0)}_{666}$ (Å^3)	0.023956	$\delta^{(0)}_{3333}$ (Å^{-1})	−0.086087
$\delta^{(0)}_{15}$ (Å^2)	−0.082276	$\delta^{(0)}_{1114}$	0.238257	$\delta^{(0)}_{3346}$ (Å)	−0.181862
$\delta^{(0)}_{44}$ (Å^3)	0.040883	$\delta^{(0)}_{1116}$	0.390058	$\delta^{(0)}_{3445}$ (Å^2)	−0.104290
$\delta^{(0)}_{45}$ (Å^3)	−0.079680	$\delta^{(0)}_{1122}$ (Å^{-1})	0.211208	$\delta^{(0)}_{3456}$ (Å^2)	0.092558
$\delta^{(0)}_{116}$ (Å)	−0.600373	$\delta^{(0)}_{1123}$ (Å^{-1})	−0.149092	$\delta^{(0)}_{3556}$ (Å^2)	0.041340
$\delta^{(0)}_{123}$	0.985018	$\delta^{(0)}_{1124}$	−0.237972	$\delta^{(0)}_{3666}$ (Å^2)	−0.040422
$\delta^{(0)}_{233}$	−0.356775	$\delta^{(0)}_{1125}$	−0.055421	$\delta^{(0)}_{4444}$ (Å^3)	0.005441
$\delta^{(0)}_{234}$ (Å)	1.092313	$\delta^{(0)}_{1126}$	−0.341766	$\delta^{(0)}_{4446}$ (Å^3)	−0.026849
$\delta^{(0)}_{235}$ (Å)	0.314545	$\delta^{(0)}_{1144}$ (Å)	0.072321	$\delta^{(0)}_{4466}$ (Å^3)	−0.109425
$\delta^{(0)}_{246}$ (Å^2)	0.391433	$\delta^{(0)}_{1155}$ (Å)	−0.067657	$\delta^{(0)}_{4556}$ (Å^3)	0.078811
$\delta^{(0)}_{266}$ (Å^2)	−0.021601	$\delta^{(0)}_{1156}$ (Å)	−0.377933		

[a] In the cgs unit system, the static polarizability tensor components have units of cm^3. We use here the related unit Å^3 = 10^{-24} cm^3.

if the indices $k', l', m', \ldots$ are obtained from $k, l, m, \ldots$ by replacing all indices 2 by 3, all indices 3 by 2, all indices 5 by 6, and all indices 6 by 5.

We have determined the values of the expansion parameters in Eq. (15), which we take to fourth-order, in a least-squares fitting to the 3×2281 *ab initio* dipole moment projections $\bar{\mu} \cdot \mathbf{e}_j$ ($j = 1, 2, 3$). We could usefully vary 113 parameters in the final fitting, which had a rms deviation of 0.00012 D. Table 2 lists the optimized parameter values. Parameters, whose absolute values were determined to be less than their standard errors in initial fittings, were constrained to zero in the final fitting and omitted from the table. Furthermore, we give in the tables only one member of each parameter pair related by Eq. (18).

For an ion such as NH_3^+, the dipole moment vector depends on the choice of origin for the axis system used to describe this vector. The parameter values in Table 2 define, together with Eqs. (10)–(18), a dipole moment vector expressed in an axis system with origin at the center of mass for $^{14}NH_3^+$. This dipole moment vector is required to calculate the line strengths of electric-dipole transitions for $^{14}NH_3^+$ (see for example, Ref. [26]).

The components of the static electric polarizability tensor $\boldsymbol{\alpha}_s$, expressed in a laboratory-fixed Cartesian axis system XYZ, are denoted by α_{AB} ($A, B = X, Y, Z$). In the *ab initio* calculations of the present work we determine electronic expectation values $\bar{\alpha}_{AB}$ (which depend on the vibrational coordinates) of these quantities in the electronic ground state. At this stage of the computation, XYZ represents the laboratory-fixed axis system used to define the nuclear positions in the *ab initio* calculation. In order to

provide a description of the polarizability tensor that is independent of the choice of axis system we utilize an MB-type representation, i.e., we express the tensor $\bar{\boldsymbol{\alpha}}_s$ in terms of the vectors $\mathbf{e}_i$ from Eq. (9):

$$\bar{\boldsymbol{\alpha}}_s = \mathbf{e}_N \bar{\delta}_0 \mathbf{e}_N + \sum_{i=1}^{3} \sum_{j=1}^{3} \mathbf{e}_i \bar{\alpha}^{Bond}_{i,j} \mathbf{e}_j \qquad (19)$$

or, equivalently, in terms of the components

$$(\bar{\boldsymbol{\alpha}}_s)_{AB} = (\mathbf{e}_N)_A \bar{\delta}_0 (\mathbf{e}_N)_B + \sum_{i=1}^{3} \sum_{j=1}^{3} (\mathbf{e}_i)_A \bar{\alpha}^{Bond}_{i,j} (\mathbf{e}_j)_B \qquad (20)$$

where $A, B = X, Y, Z$ and $\mathbf{e}_N = \mathbf{q}_N/|\mathbf{q}_N|$ with the 'trisector'

$$\mathbf{q}_N = (\mathbf{e}_1 \times \mathbf{e}_2) + (\mathbf{e}_2 \times \mathbf{e}_3) + (\mathbf{e}_3 \times \mathbf{e}_1). \qquad (21)$$

We define

$$D = \mathbf{e}_N \cdot \mathbf{e}_1 = \mathbf{e}_N \cdot \mathbf{e}_2 = \mathbf{e}_N \cdot \mathbf{e}_3 = (\mathbf{e}_1 \times \mathbf{e}_2) \cdot \mathbf{e}_3/|\mathbf{q}_N| \qquad (22)$$

and obtain in a derivation analogous to that leading to Eq. (10)

$$\bar{\alpha}^{Bond}_{i,j} = \sum_{k=1}^{3} \sum_{l=1}^{3} (\mathbf{A}^{-1})_{ik} \left[\mathbf{e}_k \cdot (\bar{\boldsymbol{\alpha}}_s \mathbf{e}_l^T) - D^2 \bar{\delta}_0 \right] (\mathbf{A}^{-1})_{lj} \qquad (23)$$

where $\mathbf{A}^{-1}$ is the matrix[2] introduced in connection with Eq. (10), the vectors $\mathbf{e}_k$ and $\mathbf{e}_l$ are understood as row (1×3) matrices, and a superscript T denotes transposition.

By analogy with Eqs. (12)–(14), we introduce parameterized functions representing the projections $\mathbf{e}_k \cdot (\bar{\boldsymbol{\alpha}}_s \mathbf{e}_l^T)$ from Eq. (23). The symmetry properties of these functions are such that we can express them in terms of two scalar functions $\bar{\alpha}_0$ and $\bar{\gamma}_0$:

$$\mathbf{e}_1 \cdot (\bar{\boldsymbol{\alpha}}_s \mathbf{e}_1^T) = \bar{\alpha}_0(r_1, r_2, r_3, \alpha_1, \alpha_2, \alpha_3)$$
$$= \bar{\alpha}_0(r_1, r_3, r_2, \alpha_1, \alpha_3, \alpha_2), \qquad (24)$$

$$\mathbf{e}_2 \cdot (\bar{\boldsymbol{\alpha}}_s \mathbf{e}_2^T) = \bar{\alpha}_0(r_2, r_3, r_1, \alpha_2, \alpha_3, \alpha_1)$$
$$= \bar{\alpha}_0(r_2, r_1, r_3, \alpha_2, \alpha_1, \alpha_3), \qquad (25)$$

$$\mathbf{e}_3 \cdot (\bar{\boldsymbol{\alpha}}_s \mathbf{e}_3^T) = \bar{\alpha}_0(r_3, r_1, r_2, \alpha_3, \alpha_1, \alpha_2)$$
$$= \bar{\alpha}_0(r_3, r_2, r_1, \alpha_3, \alpha_2, \alpha_1), \qquad (26)$$

and

$$\mathbf{e}_2 \cdot (\bar{\boldsymbol{\alpha}}_s \mathbf{e}_3^T) = \mathbf{e}_3 \cdot (\bar{\boldsymbol{\alpha}}_s \mathbf{e}_2^T) = \bar{\gamma}_0(r_1, r_2, r_3, \alpha_1, \alpha_2, \alpha_3)$$
$$= \bar{\gamma}_0(r_1, r_3, r_2, \alpha_1, \alpha_3, \alpha_2), \qquad (27)$$

$$\mathbf{e}_1 \cdot (\bar{\boldsymbol{\alpha}}_s \mathbf{e}_3^T) = \mathbf{e}_3 \cdot (\bar{\boldsymbol{\alpha}}_s \mathbf{e}_1^T) = \bar{\gamma}_0(r_2, r_3, r_1, \alpha_2, \alpha_3, \alpha_1)$$
$$= \bar{\gamma}_0(r_2, r_1, r_3, \alpha_2, \alpha_1, \alpha_3), \qquad (28)$$

$$\mathbf{e}_1 \cdot (\bar{\boldsymbol{\alpha}}_s \mathbf{e}_2^T) = \mathbf{e}_2 \cdot (\bar{\boldsymbol{\alpha}}_s \mathbf{e}_1^T) = \bar{\gamma}_0(r_3, r_1, r_2, \alpha_3, \alpha_1, \alpha_2)$$
$$= \bar{\gamma}_0(r_3, r_2, r_1, \alpha_3, \alpha_2, \alpha_1). \qquad (29)$$

Since the $\bar{\boldsymbol{\alpha}}_s$ tensor is symmetric, we have $\mathbf{e}_i \cdot (\bar{\boldsymbol{\alpha}}_s \mathbf{e}_j^T) = \mathbf{e}_j \cdot (\bar{\boldsymbol{\alpha}}_s \mathbf{e}_i^T)$ for $i \neq j$. The scalar functions $\bar{\alpha}_0$ and $\bar{\gamma}_0$ are expanded (in a manner analogous to Eq. (15)) in terms of the internal coordinates ζ_k from Eqs. (16) and (17):

[2] As mentioned above, $\mathbf{A}^{-1}$ does not exist at planarity. By analogy with the procedure used for the MB representation of the dipole moment [30,32], at planar geometries we set $\bar{\alpha}^{Bond}_{i,j} = 0$ for $i = 3$ and/or $j = 3$ and express $\bar{\boldsymbol{\alpha}}_s$ in terms of $\mathbf{e}_1, \mathbf{e}_2$, and $\mathbf{e}_N = \mathbf{e}_1 \times \mathbf{e}_2/|\mathbf{e}_1 \times \mathbf{e}_2|$ only.

Table 6
Band centers (in cm^{-1}) for vibrational states of ^{14}NH$_3^+$ with A$'_1$, A$''_2$, E$'$, and E$''$ symmetry

State[a]	Γ[b]	AQZ[c]	Obs.[d]	MR-CI[e]	CEPA[f]	State	Γ	AQZ	Obs.	MR-CI[e]
$2v_2$	A$'_1$	1836.69	1843.9	1840	1839	v_4	E$'$	1512.54	1507.1	1518
$2v_4$	A$'_1$	2998.66				$2v_4$	E$'$	3015.73		
v_1	A$'_1$	3230.87	3232[g]	3221	3322	$2v_2 + v_4$	E$'$	3368.85		3327
$4v_2$	A$'_1$	3796.11	3807.4	3794	3812	v_3	E$'$	3389.49	3388.65[h]	3331
$3v_4$	A$'_1$	4509.33				$3v_4$	E$'$	4478.28		
$2v_2 + 2v_4$	A$'_1$	4875.99				$v_1 + v_4$	E$'$	4731.49		
$v_3 + v_4$	A$'_1$	4897.52				$v_3 + v_4$	E$'$	4879.45		
$v_1 + 2v_2$	A$'_1$	5053.99				$2v_2 + 2v_4$	E$'$	4891.90		
$6v_2$	A$'_1$	5838.99	5851.7	5833	5877	$2v_2 + v_3$	E$'$	5192.20		
$4v_4$	A$'_1$	5938.25				$4v_2 + v_4$	E$'$	5345.37		
$v_1 + 2v_4$	A$'_1$	6201.72				$4v_4$	E$'$	5952.52		
$v_3 + 2v_4$	A$'_1$	6358.85				$4v_4$	E$'$	5996.56		
$2v_2 + 3v_4$	A$'_1$	6404.43				$v_1 + 2v_4$	E$'$	6220.87		
$2v_1$	A$'_1$	6404.75				$v_3 + 2v_4$	E$'$	6335.89		
$2v_3$	A$'_1$	6691.19				$2v_2 + 3v_4$	E$'$	6376.01		
$2v_2 + v_3 + v_4$	A$'_1$	6721.18				$v_3 + 2v_4$	E$'$	6381.04		
$4v_2 + 2v_4$	A$'_1$	6870.95				$v_1 + v_3$	E$'$	6515.33		
$v_1 + 4v_2$	A$'_1$	7000.12				$v_1 + 2v_2 + v_4$	E$'$	6574.90		
$\cdots$						$2v_2 + v_3 + v_4$	E$'$	6702.07		
$8v_2$	A$'_1$	7943.52	7957.8	7935	8010	$2v_3$	E$'$	6751.66		
						$4v_2 + 2v_4$	E$'$	6884.63		
v_2	A$''_2$	899.33	903.39[i]	903	899	$v_2 + v_4$	E$''$	2421.91		2413
$3v_2$	A$''_2$	2804.10	2813.2	2805	2812	$v_2 + 2v_4$	E$''$	3935.14		
$v_2 + 2v_4$	A$''_2$	3918.51				$v_2 + v_3$	E$''$	4271.49	4274.95[j]	4247
$v_1 + v_2$	A$''_2$	4123.35	4127.5[k]	4143	4214	$3v_2 + v_4$	E$''$	4345.23		4259
$5v_2$	A$''_2$	4808.74	4821.2	4804	4835	$v_2 + 3v_4$	E$''$	5408.37		
$v_2 + 3v_4$	A$''_2$	5438.43				$v_1 + v_2 + v_4$	E$''$	5634.30		
$v_2 + v_3 + v_4$	A$''_2$	5790.09				$v_2 + v_3 + v_4$	E$''$	5771.74		
$3v_2 + 2v_4$	A$''_2$	5862.01				$3v_2 + 2v_4$	E$''$	5876.74		
$v_1 + 3v_2$	A$''_2$	6014.71	6022.5[g]		6115	$3v_2 + v_3$	E$''$	6143.29		
$v_2 + 4v_4$	A$''_2$	6878.42				$5v_2 + v_4$	E$''$	6365.29		
$7v_2$	A$''_2$	6884.52	6899.4	6877	6936	$v_2 + 4v_4$	E$''$	6892.42		
$\cdots$						$v_2 + 4v_4$	E$''$	6935.53		
$9v_2$	A$''_2$	9014.58	9030.4	9007	9097					

[a] Spectroscopic assignment.
[b] Symmetry of the vibrational state in D$_{3h}$(M) [26,27].
[c] Band centers calculated theoretically in this work.
[d] Experimental band centers, from Ref. [6] unless otherwise indicated.
[e] MR-CI theoretical band centers from Ref. [21].
[f] CEPA theoretical band centers from Ref. [19].
[g] Ref. [14].
[h] Ref. [1].
[i] Ref. [2].
[j] Ref. [3].
[k] Ref. [14]. The experimental value obtained in Ref. [6] is 4345.7 cm^{-1}.

$$\bar{c}_0 = c_0^{(0)} + \sum_k c_k^{(0)} \zeta_k + \sum_{k,l} c_{kl}^{(0)} \zeta_k \zeta_l + \sum_{k,l,m} c_{klm}^{(0)} \zeta_k \zeta_l \zeta_m + \sum_{k,l,m,n} c_{klmn}^{(0)} \zeta_k \zeta_l \zeta_m \zeta_n \quad (30)$$

with $c = \alpha$ and γ, respectively. The expansion coefficients $\alpha_{klm\ldots}^{(0)}$ (for $c = \alpha$) and $\gamma_{klm\ldots}^{(0)}$ (for $c = \gamma$) in Eq. (30) are subject to the permutation rules given in Eq. (18). We have determined the values of the expansion coefficients $\alpha_{klm\ldots}^{(0)}$ and $\gamma_{klm\ldots}^{(0)}$ defined by Eq. (30) for $c = \alpha$ and γ, respectively, in least-squares fittings to polarizability tensor component values calculated *ab initio* for NH$_3^+$. For $\bar{\alpha}_0$, we fitted 3×2661 data points and achieved an rms deviation of 0.000083 Å^3 by varying the 109 parameters whose opti-

mized values are listed in Table 3. For $\bar{\gamma}_0$, we also fitted 7983 data points by varying 107 parameters (Table 4). The rms deviation of the final fitting was 0.000068 Å^3. Parameters, whose values are not listed in Tables 3 and 4, were constrained to zero in the final fittings.

The term $\mathbf{e}_N \bar{\delta}_0 \mathbf{e}_N$ in Eq. (19) is required in order to describe correctly the polarizability tensor components at planar configurations. When the molecule is planar, the three vectors $\mathbf{e}_1$, $\mathbf{e}_2$, $\mathbf{e}_3$ (Eq. (9)) all lie in the molecular plane. If, for the planar configuration, we consider an axis system xyz with the x and y axes in the molecular plane and the z axis perpendicular to it, then the term involving the $\bar{\alpha}_{i,j}^{\text{Bond}}$-functions in Eq. (19) will, by necessity, produce zero contributions to the $\bar{\alpha}_s$-components $\alpha_{xz} = \alpha_{zx}$, $\alpha_{yz} = \alpha_{zy}$, and α_{zz} at

Table 7
Vibrational transition moments μ_{fi} for $^{14}NH_3^+$ (in D)

States		μ_{fi}		
i	f	MR-CI[a]	CEPA[b]	ATZfc[c]
g.s.	v_2	0.311	0.324	0.318
v_2	$2v_2$		0.440	0.434
$2v_2$	$3v_2$		0.525	0.517
$3v_2$	$4v_2$		0.591	0.583
$4v_2$	$5v_2$		0.645	0.638
$5v_2$	$6v_2$		0.694	0.686
$6v_2$	$7v_2$		0.735	0.728
$7v_2$	$8v_2$		0.775	0.766
$8v_2$	$9v_2$		0.807	0.801
v_2	v_1			0.031
g.s.	v_3	0.238		0.248
v_2	$v_2 + v_3$			0.243
g.s.	v_4	0.187		0.185
v_2	$v_2 + v_4$			0.182
g.s.	$2v_2 + v_4$			0.007
v_2	$3v_2 + v_4$			0.008
g.s.	$2v_4^2$			0.036
v_2	$v_2 + 2v_4^2$			0.038

[a] MR-CI theoretical values from Ref. [23].
[b] CEPA theoretical values from Ref. [18].
[c] Present work.

Table 8
Vibrational transition moments μ_{fi} and effective intensities $\bar{I}_{fi}$ ($T=300$ K) for $^{14}NH_3^+$ transitions originating in the ground vibrational state

Band[a]	Γ_f[b]	v_{fi} (cm^{-1})	μ_{fi} (D)	$\bar{I}_{fi}$ (cm mol^{-1})
v_2	A_2''	899.33	0.31746	224,140.9
v_4	E'	1512.54	0.18478	129,360.6
$3v_2$	A_2''	2804.10	0.00067	3.1
$2v_4$	E'	3015.73	0.03626	9937.5
$2v_2 + v_4$	E'	3368.85	0.00743	465.7
v_3	E'	3389.49	0.24759	520,816.7
$v_2 + 2v_4$	A_2''	3918.51	0.00062	3.8
$v_1 + v_2$	A_2''	4123.35	0.01418	2078.6
$3v_4$	E'	4478.28	0.00135	20.5
$v_1 + v_4$	E'	4731.49	0.00274	89.1
$v_3 + v_4$	E'	4879.45	0.03072	11,546.3
$2v_2 + 2v_4$	E'	4891.90	0.00313	119.8
$2v_2 + v_3$	E'	5192.20	0.00383	190.8
$v_2 + 3v_4$	A_2''	5438.43	0.00074	7.4
$v_2 + v_3 + v_4$	A_2''	5790.09	0.00070	7.2
$4v_4$	E'	5952.52	0.00072	7.7
$4v_4$	E'	5996.56	0.00097	14.2
$v_1 + 2v_4$	E'	6220.87	0.00222	77.1
$v_3 + 2v_4$	E'	6335.89	0.00479	363.9
$v_3 + 2v_4$	E'	6381.04	0.00053	4.5
$v_1 + v_3$	E'	6515.33	0.01869	5703.8
$2v_2 + v_3 + v_4$	E'	6702.07	0.00042	3.0
$2v_3$	E'	6751.66	0.00505	431.2
$v_2 + v_3 + 2v_4$	A_2''	7259.86	0.00045	3.6
$2v_1 + v_2$	A_2''	7290.40	0.00109	21.5
$v_1 + 3v_4$	E'	7663.79	0.00056	6.0
$v_3 + 3v_4$	E'	7793.37	0.00041	3.4
$2v_1 + v_4$	E'	7894.21	0.00100	19.9
$v_1 + v_3 + v_4$	E'	7996.52	0.00249	124.1
$2v_3 + v_4$	E'	8162.96	0.00089	16.2
$2v_3 + v_4$	E'	8233.26	0.00103	22.0
$v_1 + 2v_2 + v_3$	E'	8304.08	0.00047	4.6
$2v_1 + 2v_4$	E'	9368.53	0.00083	16.0
$v_1 + v_3 + 2v_4$[c]	E'	9435.96	0.00053	6.7
$2v_1 + v_3$[c]	E'	9557.14	0.00176	74.5
$v_1 + 2v_3$[c]	E'	9819.33	0.00076	14.3
$3v_3$[c]	E'	9970.07	0.00147	53.7
$3v_3 + v_4$[c]	E'	11,491.38	0.00069	13.9
$3v_3 + 2v_4$[c]	E'	12,942.49	0.00065	13.6
$4v_3$[c]	E'	13,184.39	0.00030	3.0

[a] Spectroscopic assignment.
[b] Symmetry of the final vibrational state in $D_{3h}(M)$.
[c] Ambiguous assignment. The use of un-symmetrized stretching basis functions makes it difficult to assign v_1 and v_3 unambiguously.

planarity. By symmetry [26], the components $\alpha_{xz} = \alpha_{zx}$ and $\alpha_{yz} = \alpha_{zy}$ vanish at planarity and no problem arises, but α_{zz} is non-zero at planarity, and we have introduced the term $\mathbf{e}_N\bar{\delta}_0\mathbf{e}_N$ in Eq. (19) to model it. For planar geometries, the unit vector $\mathbf{e}_N$ is perpendicular to the molecular plane so that we have $\bar{\delta}_0 = \bar{\alpha}_{zz}$. We represent $\bar{\delta}_0$ as an expansion in terms of the internal coordinates ζ_k from Eqs. (16) and (17); see Eq. (30) with $c = \delta$. Values of the corresponding expansion coefficients $\delta_{klm...}^{(0)}$ are obtained by fitting the expansion through values of the projection $\mathbf{e}_N \cdot (\bar{\boldsymbol{\alpha}}_s\mathbf{e}_N^T)$ which, at planar geometries, has the value $\bar{\alpha}_{zz}$. The scalar function $\bar{\delta}_0$ depends on the coordinates $r_1, r_2, r_3, \alpha_1, \alpha_2$, and α_3 and is totally symmetric in $D_{3h}(M)$. Consequently, the expansion coefficients $\delta_{klm...}^{(0)}$ (Eq. (30) with $c = \delta$) are subject to symmetry constraints which we can express as

$$\delta_{k'l'm'...}^{(0)} = \delta_{klm...}^{(0)} \tag{31}$$

For example, in order that $\bar{\delta}_0$ be invariant under the operation (123) of $D_{3h}(M)$ [26], the indices $k'l'm'...$ in Eq. (31) are obtained from $klm...$ when all indices 1 are replaced by 3, all indices 2 by 1, all indices 3 by 2, all indices 4 by 6, all indices 5 by 4, and all indices 6 by 5. Similar relations can be obtained by considering the other permutation operations (132), (12), (13), and (23) in $D_{3h}(M)$. With the 46 unique parameters listed in Table 5 we were able to reproduce 2661 ab initio values of $\mathbf{e}_N \cdot (\bar{\boldsymbol{\alpha}}_s\mathbf{e}_N^T)$ with an rms deviation of 0.000050 Å^3. At equilibrium we obtain $\bar{\delta}_{(0)} = -0.8868$ Å^3. At the planar equilibrium geometry (with all $\alpha_i = 120°$ and all $r_i = r_e = 1.0207$ Å), the polarizability tensor of NH_3^+ is characterized by $\bar{\alpha}_e^{(0)} \equiv \bar{\alpha}_0(r_e, r_e, r_e, 120°, 120°, 120°) = -1.2060$ Å^3, $\bar{\gamma}_0(r_e, r_e, r_e, 120°, 120°, 120°) = -\bar{\alpha}_e^{(0)}/2$, and $\bar{\delta}_e^{(0)} = \bar{\delta}_0(r_e, r_e, r_e, 120°, 120°, 120°) = -0.8868$ Å^3. If

we choose, as in the preceding paragraph, a molecule-fixed axis system xyz such that the z-axis is perpendicular to the molecular plane at equilibrium, the only non-zero components are $\bar{\alpha}_{xx}^{(m)} = \bar{\alpha}_{yy}^{(m)} = \bar{\alpha}_e^{(0)}$, and $\bar{\alpha}_{zz}^{(m)} = \bar{\delta}_e^{(0)}$.

The intensity of a Raman transition depends on matrix elements of static polarizability tensor components between the ro-vibrational wavefunctions connected by the transition [26,27,54]. The static polarizability tensor determines the electric-dipole moment induced by an external electric field. In order to facilitate the evaluation of the matrix elements required for computing Raman intensities, the Cartesian polarizability tensor is conveniently transformed to irreducible spherical tensor form [26,54]. The irreducible

Table 9
Vibrational transition moments μ_{fi} and effective intensities $\bar{I}_{\mathrm{fi}}$ ($T = 300$ K) for a number of hot $^{14}\mathrm{NH}_3^+$ transitions

Band[a]	Γ_i[b]	Γ_f[c]	ν_{fi} (cm^{-1})	μ_{fi} (D)	$\bar{I}_{\mathrm{fi}}$ (cm mol^{-1})
$2\nu_2 - \nu_2$	A_2''	A_1'	937.37	0.43392	5858.6
$\nu_2 + \nu_4 - \nu_2$	A_2''	E''	1522.59	0.18174	1687.0
$2\nu_4 - \nu_2$	A_2''	A_1'	2099.33	0.01049	7.8
$\nu_1 - \nu_2$	A_2''	A_1'	2331.55	0.03134	76.9
$\nu_2 + 2\nu_4 - \nu_2$	A_2''	E''	3035.81	0.03791	146.5
$\nu_2 + \nu_3 - \nu_2$	A_2''	E''	3372.17	0.24340	6706.5
$3\nu_2 + \nu_4 - \nu_2$	A_2''	E''	3445.90	0.00756	6.6
$\nu_1 + 2\nu_2 - \nu_2$	A_2''	A_1'	4154.66	0.01913	51.0
$\nu_2 + \nu_3 + \nu_4 - \nu_2$	A_2''	E''	4872.42	0.03059	153.0
$3\nu_2 + \nu_3 - \nu_2$	A_2''	E''	5243.96	0.00610	6.6
$\nu_2 + \nu_3 + 2\nu_4 - \nu_2$	A_2''	E''	6340.09	0.00560	6.7
$\nu_1 + \nu_2 + \nu_3 - \nu_2$	A_2''	E''	6490.76	0.01835	73.4
$\nu_2 + 2\nu_3 - \nu_2$	A_2''	E''	6717.97	0.00467	4.9
$\nu_2 + \nu_4 - \nu_4$	E'	E''	909.37	0.45232	325.7
$2\nu_4 - \nu_4$	E'	A_1'	1486.12	0.18957	94.6
$2\nu_4 - \nu_4$	E'	E'	1503.19	0.25875	178.3
$\nu_1 - \nu_4$	E'	A_1'	1718.33	0.03508	3.7
$\nu_3 - \nu_4$	E'	E'	1876.95	0.05928	11.7
$3\nu_4 - \nu_4$	E'	E'	2965.73	0.02695	3.8
$3\nu_4 - \nu_4$	E'	A_1'	2996.78	0.04314	9.9
$3\nu_4 - \nu_4$	E'	A_2'	2998.48	0.04517	10.8
$\nu_1 + \nu_4 - \nu_4$	E'	E'	3218.95	0.02651	4.0
$\nu_3 + \nu_4 - \nu_4$	E'	A_2'	3358.92	0.17512	182.6
$\nu_3 + \nu_4 - \nu_4$	E'	E'	3366.90	0.22848	311.6
$2\nu_2 + 2\nu_4 - \nu_4$	E'	E'	3379.35	0.03231	6.3
$\nu_3 + \nu_4 - \nu_4$	E'	A_1'	3384.98	0.16719	167.8
$\nu_1 + \nu_2 + \nu_4 - \nu_4$	E'	E''	4121.76	0.02030	3.0
$\nu_3 + 2\nu_4 - \nu_4$	E'	E'	4823.34	0.02998	7.7
$\nu_3 + 2\nu_4 - \nu_4$	E'	A_1'	4846.30	0.03393	9.9
$\nu_3 + 2\nu_4 - \nu_4$	E'	A_2'	4848.88	0.03201	8.8
$2\nu_1 + \nu_4 - \nu_4$	E'	E'	6483.97	0.01795	3.7
$3\nu_2 - 2\nu_2$	A_1'	A_2''	967.41	0.51678	95.8
$2\nu_2 + \nu_4 - 2\nu_2$	A_1'	E'	1532.16	0.17859	18.3
$2\nu_2 + \nu_3 - 2\nu_2$	A_1'	E'	3355.51	0.23979	72.3
$2\nu_2 + \nu_4 - (\nu_2 + \nu_4)$	E''	E'	946.94	0.61774	8.1
$\nu_2 + \nu_3 + \nu_4 - (\nu_2 + \nu_4)$	E''	E'	3349.83	0.22681	3.9

[a] Spectroscopic assignment of the vibrational band.
[b] Symmetry of the initial vibrational state in D$_{3h}$(M).
[c] Symmetry of the final vibrational state in D$_{3h}$(M).

tensor components of the static electric polarizability tensor in the space-fixed axis system are

$$\bar{\alpha}_s^{(0,0)} = -\frac{1}{\sqrt{3}}\left[\bar{\alpha}_{XX} + \bar{\alpha}_{YY} + \bar{\alpha}_{ZZ}\right] \tag{32}$$

$$\bar{\alpha}_s^{(2,0)} = \frac{1}{\sqrt{6}}\left[2\bar{\alpha}_{ZZ} - \bar{\alpha}_{XX} - \bar{\alpha}_{YY}\right] \tag{33}$$

$$\bar{\alpha}_s^{(2,\pm1)} = \mp\bar{\alpha}_{XZ} - i\bar{\alpha}_{YZ} \tag{34}$$

$$\bar{\alpha}_s^{(2,\pm2)} = \frac{1}{2}\left[\bar{\alpha}_{XX} - \bar{\alpha}_{YY}\right] \pm i\bar{\alpha}_{XY} \tag{35}$$

where we use a 'bar' to signify that the tensor components are averaged over the electronic ground state wavefunction. The space-fixed components $\bar{\alpha}_s^{(\sigma,\sigma')}$ can now be relatively straightforwardly transformed to the molecule-fixed axis system xyz [26,55]. The operator $\bar{\alpha}_s^{(0,0)}$ in Eq. (32) is

totally symmetric in the rotation group $\boldsymbol{K}$ (spatial) [26] and thus invariant under rotations in space (i.e., it transforms as the irreducible representation $D^{(0)}$). The operators $\bar{\alpha}_s^{(2,\sigma)}$, $\sigma = 0, \pm1, \pm2$, in Eqs. (33)–(35) transform as the irreducible representation $D^{(2)}$ of the group $\boldsymbol{K}$ (spatial). The irreducible tensor components in the molecule-fixed axis system xyz, which we denote as $\bar{\alpha}_m^{(0,0)}$, $\bar{\alpha}_m^{(2,0)}$, $\bar{\alpha}_m^{(2,\pm1)}$, and $\bar{\alpha}_m^{(2,\pm2)}$, are obtained [26,56] by replacing, in Eqs. (32)–(35), subscript s by subscript m, X by x, Y by y, and Z by z.

4. Rotation–vibration energies and spectra

4.1. Band centers

The AQZ potential energy surface described in Section 2 has been used to calculate vibrational term values of $^{14}\mathrm{NH}_3^+$. The calculations were carried out with the computer program XY3 described in detail previously [29]. In the numerical integration of the out-of-plane-bending Schrödinger equation (see Ref. [29]) a grid of 1000 points was used. The size of the vibrational basis set was controlled by the parameter $P_{\max}$ defined so that

$$P = 2(v_1 + v_3) + v_2/2 + v_4 \leqslant P_{\max}, \tag{36}$$

where the vibrational quantum numbers v_1, v_3 are associated with the stretching basis functions, v_2 describes the excitation of the out-of-plane bending mode, and v_4 describes the excitation of the 'deformation' bending mode. We use here $P_{\max} = 14$. The kinetic energy operator expansion was truncated after the fourth-order terms while the potential energy function was truncated after the sixth-order terms [29]. The spin-rotation splitting is found to be small for NH$_3^+$ [1] and so we neglect spin effects in the rovibrational calculations. In Table 6, we list the calculated term values for vibrational states of $^{14}\mathrm{NH}_3^+$ with A_1', A_2'', E', and E'' symmetry in D$_{3h}$(M) (states of symmetry A_2' and A_1'' are highly excited and no such state has been experimentally characterized owing to unfavourable selection rules); the calculated term values are compared with the available experimental and theoretical values. Calculations carried out with the kinetic energy operator being expanded to different orders suggest that for the term values in Table 6, the error originating in the kinetic energy truncation is generally within 1 cm^{-1}. The only exception is the $v_2 + 4v_4$ level at 6878.42 cm^{-1} which has an estimated error of about 3 cm^{-1}.

4.2. Electric-dipole transition moments

Along with the band centers described in Section 4.1 we compute the vibrational transition moments defined as

$$\mu_{\mathrm{fi}} = \sqrt{\sum_{\alpha = x,y,z}\left|\left\langle \Phi_{\mathrm{vib}}^{(\mathrm{f})}|\bar{\mu}_\alpha|\Phi_{\mathrm{vib}}^{(\mathrm{i})}\right\rangle\right|^2}, \tag{37}$$
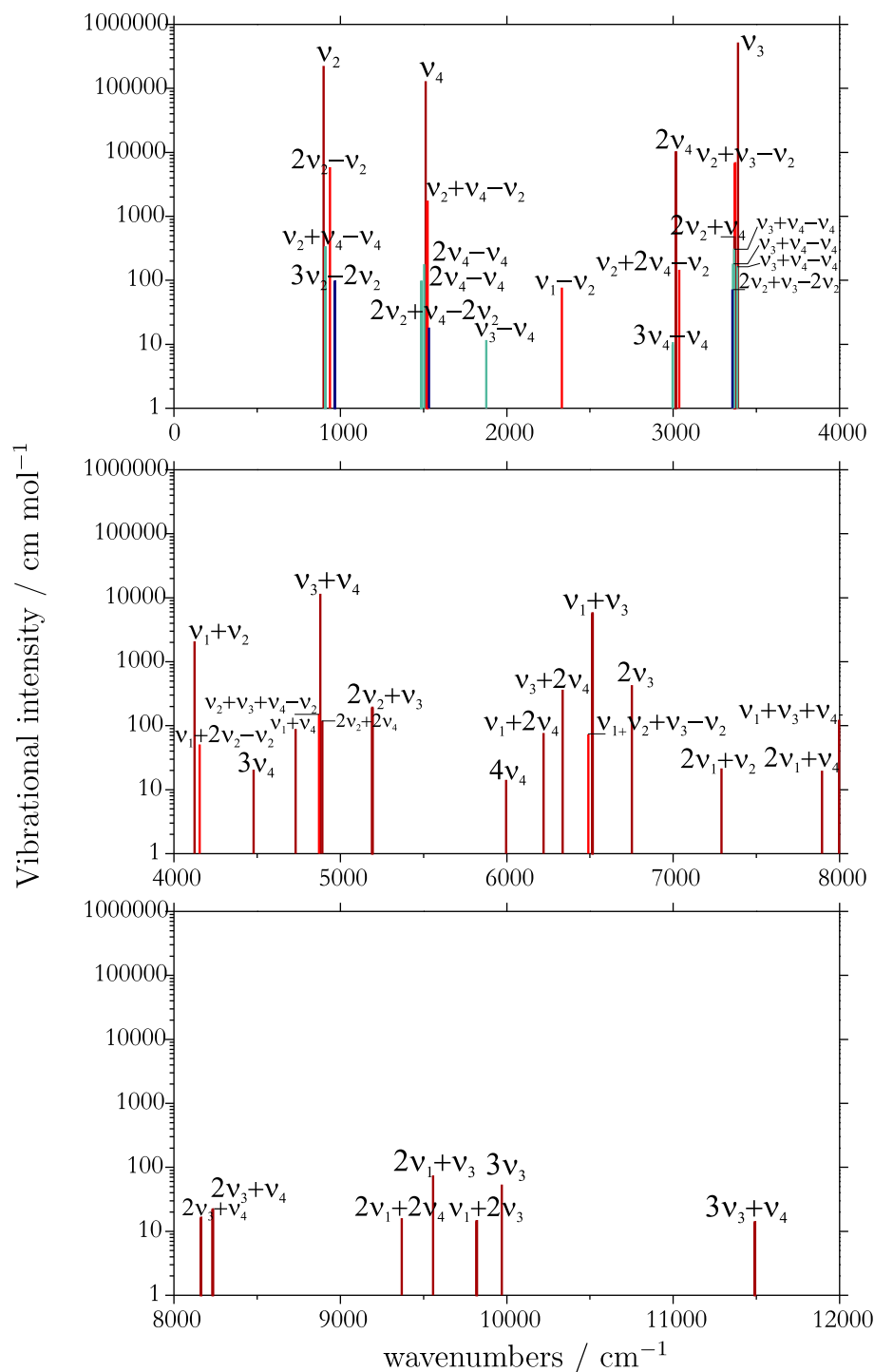
Fig. 1. 'Effective' absorption intensities of $^{14}NH_3^+$ computed at an absolute temperature of 300 K (note the logarithmic ordinate scale and see the text for details). Only transitions with an effective intensity larger than 10 cm mol^{-1} are shown.

where $|\Phi_{vib}^{(w)}>$, $w = i$ or f, are vibrational wavefunctions ($J = 0$), and $\bar{\mu}_\alpha$ is the component of $\bar{\mu}$ (Eq. (8)) along the molecule-fixed α ($=x, y, z$) axis. The matrix elements required are generated by techniques described in Ref. [29] for matrix elements of the potential energy function. In calculating the vibrational wavefunctions, we use the *ab initio* AQZ potential energy surface. To obtain the vibrational transition moments we utilize the ATZfc dipole moment surface. The basis set truncation parameter P_{max} (Eq. (36)) was chosen to be 14.

By comparing our theoretical values for the vibrational transition moments μ_{fi} to other theoretical values available in the literature [18,23] for $^{14}NH_3^+$, we can assess the quality of the ATZfc dipole moment surface. We make this comparison in Table 7. It is seen that the ATZfc DMS affords a reasonable description of the intensities for transitions

Table 10
Matrix elements of the polarizability tensor (in Å³) for $^{14}NH_3^+$ transitions originating in the ground vibrational state

Band[a]	Γ_f[b]	ν_{fi} (cm⁻¹)	α_{00}	α_{20}	β	γ
g.s.	A'₁		1.99927	0.29718		
ν_4	E'	1512.54			0.03804	
$2\nu_2$	A'₁	1836.69	0.00125	0.00528		
$\nu_2+\nu_4$	E''	2421.91				0.00763
$2\nu_4$	E'	3015.73			0.01337	
ν_1	A'₁	3230.87	0.16195	0.06433		
$2\nu_2+\nu_4$	E'	3368.85			0.00298	
ν_3	E'	3389.49			0.07435	
$4\nu_2$	A'₁	3796.11	0.00054	0.00007		
$\nu_2+2\nu_4$	E''	3935.14				0.00067
$\nu_2+\nu_3$	E''	4271.49				0.01056
$3\nu_2+\nu_4$	E''	4345.23				0.00013
$3\nu_4$	A'₁	4509.33	0.00001	0.00029		
$\nu_1+\nu_4$	E'	4731.49			0.00567	
$\nu_3+\nu_4$	E'	4879.45			0.00708	
$2\nu_2+2\nu_4$	E'	4891.90			0.00105	
$\nu_3+\nu_4$	A'₁	4897.52	0.00307	0.00237		
$\nu_1+2\nu_2$	A'₁	5053.99	0.00029	0.00109		
$2\nu_2+\nu_3$	E'	5192.20			0.00026	
$4\nu_2+\nu_4$	E'	5345.37			0.00003	
$\nu_1+\nu_2+\nu_4$	E''	5634.30				0.00084
$\nu_2+\nu_3+\nu_4$	E''	5771.74				0.00009
$3\nu_2+2\nu_4$	E''	5876.74				0.00028
$4\nu_4$	E'	5996.56			0.00016	
$\nu_1+2\nu_4$	E'	6220.87			0.00054	
$\nu_3+2\nu_4$	A'₁	6358.85	0.00092	0.00012		
$5\nu_2+\nu_4$	E''	6365.29				0.00006
$\nu_3+2\nu_4$	E'	6381.04			0.00019	
$2\nu_2+3\nu_4$	A'₁	6404.43	0.00028	0.00025		
$2\nu_1$	A'₁	6404.75	0.00149	0.00158		
$\nu_1+\nu_3$	E'	6515.33			0.00108	
$\nu_1+2\nu_2+\nu_4$	E'	6574.90			0.00006	
$2\nu_3$	A'₁	6691.19	0.00580	0.00202		
$2\nu_2+\nu_3+\nu_4$	E'	6702.07			0.00021	
$2\nu_2+\nu_3+\nu_4$	A'₁	6721.18	0.00008	0.00027		
$2\nu_3$	E'	6751.66			0.00261	
$\nu_2+4\nu_4$	E''	6935.53				0.00002
$\nu_1+4\nu_2$	A'₁	7000.12	0.00002	<10⁻⁶		

[a] Spectroscopic assignment of the vibrational band.
[b] Symmetry of the final vibrational state in $D_{3h}(M)$.

Table 11
Matrix elements of the polarizability tensor (in Å³) for a number of hot $^{14}NH_3^+$ transitions

Band[a]	Γ_f[b]	Γ_i[c]	ν_{fi} (cm⁻¹)	α_{00}	α_{20}	β	γ
$\nu_2-\nu_2$	A''₂	A''₂	0.00	2.00693	0.29368		
$\nu_4-\nu_2$	E'	A''₂	613.22				0.00766
$\nu_2+\nu_4-\nu_2$	E''	A''₂	1522.59			0.03826	
$3\nu_2-\nu_2$	A''₂	A''₂	1904.77	0.00283	0.00955		
$2\nu_4-\nu_2$	E'	A''₂	2116.41				0.00069
$2\nu_2+\nu_4-\nu_2$	E'	A''₂	2469.53				0.01096
$\nu_3-\nu_2$	E'	A''₂	2490.17				0.01023
$\nu_2+2\nu_4-\nu_2$	E''	A''₂	3035.81			0.01387	
$\nu_2+\nu_3-\nu_2$	E''	A''₂	3372.17			0.07460	
$3\nu_2+\nu_4-\nu_2$	E''	A''₂	3445.90			0.00096	
$\nu_1+\nu_4-\nu_2$	E'	A''₂	3832.17				0.00130
$5\nu_2-\nu_2$	A''₂	A''₂	3909.41	0.00085	0.00018		
$\nu_3+\nu_4-\nu_2$	E'	A''₂	3980.12				0.00033
$2\nu_2+2\nu_4-\nu_2$	E'	A''₂	3992.57				0.00154
$\nu_4-\nu_4$	E'	E'	0.00	2.84398	0.42642	0.00116	
$\nu_2+\nu_4-\nu_4$	E''	E'	909.37				0.00013
$2\nu_2-2\nu_2$	A'₁	A'₁	0.00	2.01463	0.29015		
$4\nu_2-2\nu_2$	A'₁	A'₁	1959.42	0.00482	0.01394		
$3\nu_2-3\nu_2$	A''₂	A''₂	0.00	2.02240	0.28666		
$5\nu_2-3\nu_2$	A''₂	A''₂	2004.64	0.00718	0.01845		
$2\nu_4-2\nu_4$	E'	E'	0.00	2.86416	0.43376	0.00044	
$\nu_1-\nu_1$	A'₁	A'₁	0.00	2.05688	0.32319		
$\nu_3-\nu_1$	E'	A'₁	158.62			0.02964	
$\nu_2+\nu_3-\nu_1$	E''	A'₁	1040.62				0.00421
$\nu_3-\nu_3$	E'	E'	0.00	2.90156	0.45125	0.02348	
$\nu_1+\nu_2-\nu_3$	A''₂	E'	733.85				0.00350
$\nu_2+\nu_3-\nu_3$	E''	E'	882.00				0.00452
$4\nu_2-4\nu_2$	A'₁	A'₁	0.00	2.03027	0.28324		
$6\nu_2-4\nu_2$	A'₁	A'₁	2042.89	0.00987	0.02305		

[a] Spectroscopic assignment of the vibrational band.
[b] Symmetry of the final vibrational state in $D_{3h}(M)$.
[c] Symmetry of the initial vibrational state in $D_{3h}(M)$.

involving both stretching and bending excitation. The corresponding vibrational transition moments for NH₃ have been reported in Refs. [30,32].

In Tables 8 and 9 we provide more extensive lists of transition moments relevant for the room-temperature absorption spectrum of $^{14}NH_3^+$. We list 'effective intensities' defined as

$$\bar{I}_{fi}(f \leftarrow i) = \frac{8\pi^3 N_A \tilde{\nu}_{if}}{(4\pi\epsilon_0)3hc} \frac{e^{-E_i/kT}}{Q_{eff}} \left[1 - e^{-(E_f-E_i)/kT}\right] \mu_{fi}^2, \quad (38)$$

where E_i and E_f are the band centers of the initial and final states, respectively, N_A is the Avogadro constant, h is Planck's constant, c is the speed of light in vacuum, k is the Boltzmann constant, $T = 300$ K, ϵ_0 is the permittivity of free space. The vibrational strength is μ_{fi}^2 with μ_{fi} defined

in Eq. (37) and, finally, the partition function Q_{eff} was set to 100. $Q_{eff} = 100$ can be viewed as a typical value of the rotation–vibration partition function, and so the value of $\bar{I}_{fi}(f \leftarrow i)$ is representative for the intensities of the individual rotation–vibration transitions of the vibrational band in question. Only transitions with $\bar{I}_{fi}(f \leftarrow i) \geqslant 3$ cm mol⁻¹ are included in Tables 8 and 9. The intensities from these tables are visualized in Fig. 1.

We have carried out calculations of the electric-dipole matrix elements in Table 7 and the effective intensities in Tables 8 and 9 (and of the polarizability tensor matrix elements described in Section 4.3 below) with various values of P_{max} (Eq. (36)). These calculations suggest that, with the limited number of significant digits given here, the values listed are essentially converged.

4.3. Polarizability tensor matrix elements

The ATZfc polarizability tensor surface has been used, together with the vibrational wavefunctions $|\Phi_{vib}^{(w)}\rangle$, $w = i$ or f, described in Section 4.2, to compute the matrix elements

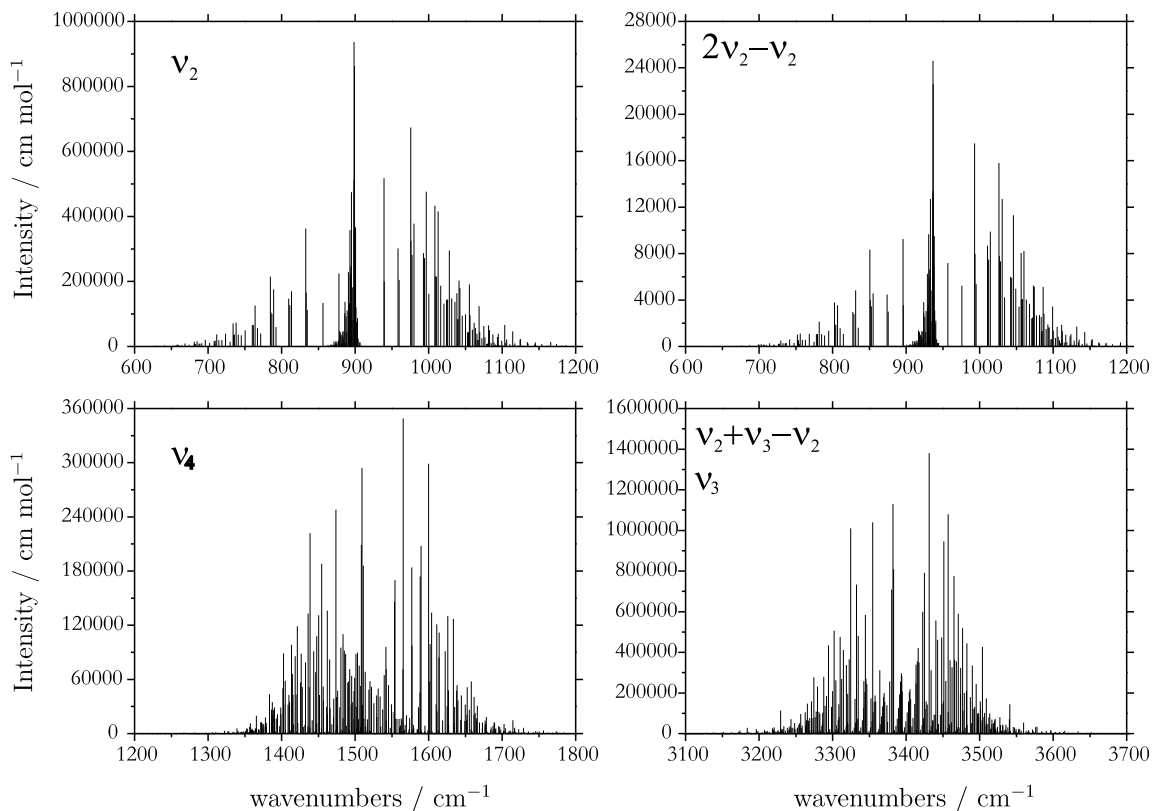Fig. 2. The ν_2, $2\nu_2 - \nu_2$, ν_3, $\nu_2 + \nu_3 - \nu_2$, and ν_4 absorption bands of $^{14}NH_3^+$, simulated at an absolute temperature of 300 K.

$$\alpha_{00}(f, i) = \sqrt{\left\langle \Phi_{vib}^{(f)} \left| \bar{\alpha}_m^{(0,0)} \right| \Phi_{vib}^{(i)} \right\rangle^2}, \tag{39}$$

$$\alpha_{20}(f, i) = \sqrt{\left\langle \Phi_{vib}^{(f)} \left| \bar{\alpha}_m^{(2,0)} \right| \Phi_{vib}^{(i)} \right\rangle^2}, \tag{40}$$

$$\beta(f, i) = \sqrt{\left\langle \Phi_{vib}^{(f)} \left| \bar{\alpha}_m^{(2,1)} \right| \Phi_{vib}^{(i)} \right\rangle^2 + \left\langle \Phi_{vib}^{(f)} \left| \bar{\alpha}_m^{(2,-1)} \right| \Phi_{vib}^{(i)} \right\rangle^2}, \tag{41}$$

$$\gamma(f, i) = \sqrt{\left\langle \Phi_{vib}^{(f)} \left| \bar{\alpha}_m^{(2,2)} \right| \Phi_{vib}^{(i)} \right\rangle^2 + \left\langle \Phi_{vib}^{(f)} \left| \bar{\alpha}_m^{(2,-2)} \right| \Phi_{vib}^{(i)} \right\rangle^2}, \tag{42}$$

where the definitions of the irreducible tensor components of the static polarizability tensor in the molecule-fixed axis system xyz, $\bar{\alpha}_m^{(0,0)}$, $\bar{\alpha}_m^{(2,0)}$, $\bar{\alpha}_m^{(2,\pm1)}$, and $\bar{\alpha}_m^{(2,\pm2)}$, are given in connection with Eqs. (32)–(35). From the matrix elements in Eqs. (39)–(42) we can generate all the vibrational matrix elements that govern the intensities of Raman transitions. The results for a number of low-wavenumber vibrational transitions are given in Tables 10 and 11.

4.4. Intensity simulations

We have simulated the ν_2, $2\nu_2 - \nu_2$, ν_3, $\nu_2 + \nu_3 - \nu_2$, and ν_4 absorption bands of $^{14}NH_3^+$ at an absolute temperature of $T = 300$ K. These simulations are based on the potential energy surface AQZ and the dipole moment surface ATZfc; they are analogous to those reported for NH_3 in Ref. [32]. The simulated bands all start in the vibrational ground state, and we include in them transitions between

rotational states with $J \leqslant 20$. In Fig. 2, we have drawn the simulated spectra as stick diagrams, where the height of the stick representing a line is the integrated absorption coefficient [30,32]. The line strengths are computed with the spin statistical weight factors $g_{ns} = 0$ for states with A_1' and A_1'' symmetry in $D_{3h}(M)$ [26,27], $g_{ns} = 12$ for states with A_2' and A_2'' symmetry, and $g_{ns} = 6$ for states with symmetry E' and E''. In order to reduce the size of the matrices to be diagonalized and thus make the calculations feasible, the vibrational basis set is reduced to have $P_{max} = 10$ (Eq. (36)) relative to the $P_{max} = 14$ basis set employed for calculating the vibrational transition moments in Section 4.2. Test calculations indicate that the effect of this reduction on the line intensity values of the bands in question is less than 0.01% and thus very small.

In computing the integrated absorption coefficient, we use the partition function value $Q = 901.2$, which is obtained from the $J \leqslant 20$ term values calculated variationally at $T = 300$ K.

5. Conclusions

We have calculated a six-dimensional CCSD(T)/aug-cc-pVQZ potential energy surface for the electronic ground state of $^{14}NH_3^+$ together with the corresponding CCSD(T)/aug-cc-pVTZ dipole moment and polarizability surfaces. The computed *ab initio* data are provided as supplementary material together with FORTRAN routines for

evaluating the corresponding analytical functions at any geometry. Based on the electronic properties, we have calculated band centers, electric-dipole transition moments, and vibrational matrix elements of the polarizability tensor components for $^{14}NH_3^+$. The rotation–vibration energies and wavefunctions employed in the latter calculations were generated by means of a variational formalism already applied to other XY_3 pyramidal molecules such as ammonia and phosphine [29,30]. Furthermore, we have used this formalism to simulate the v_2, v_3, v_4, $2v_2 - v_2$, and $v_2 + v_3 - v_2$ absorption bands of $^{14}NH_3^+$.

The vibrational term values for $^{14}NH_3^+$ (Table 6) obtained from the AQZ PES of the present work are, on the average, in substantially better agreement with experiment than the results of previous theoretical calculations [19,21] also included in Table 6 and based on PESs from CEPA [19] and MR-CI [21] *ab initio* calculations. For example, the v_3 fundamental term value is experimentally determined [1] as 3388.65 cm^{-1} and we obtain a theoretical value of 3389.49 cm^{-1} while the MR-CI calculation of Ref. [21] yielded 3331 cm^{-1}. In the CEPA calculation [19], only term values for vibrational states of A_1' or A_2'' symmetry were calculated, and so no value for the v_3 state (of E' symmetry) was given. Similarly, for the $v_1 + v_2$ state (of A_2'' symmetry), the experimental term value [14] is 4127.5 cm^{-1}, the value obtained of the present work is 4123.35 cm^{-1}, the MR-CI value [21] is 4143 cm^{-1}, and the CEPA value [19] is 4214 cm^{-1}. For a few low-lying states, the term values from the previous calculations [19,21] are in slightly better agreement with experiment than the results of the present work, but for several states at higher energy there are very significant improvements as exemplified here. Obviously the AQZ PES of the present work is a decisive improvement on the MR-CI and CEPA PESs from Refs. [19,21] and, as mentioned in Section 1, we hope that our ATZfc electric-dipole moment surface represents a similar improvement so that we can obtain accurate theoretical predictions of transition intensities, especially for transitions involving highly excited states.

We have discussed in Section 1 that to a large extent, the motivation for the present work is to facilitate the observation of NH_3^+ in an astrophysical context. A prerequisite for the observation of NH_3^+ in space is the availability of laboratory spectroscopic data and, as mentioned in Section 1, these data are very limited at the moment. We hope that the present work will stimulate further experimental studies of NH_3^+. However it should be mentioned that in general, the rovibrational transitions of the ion are found theoretically to be quite weak, and this makes the observation in space a challenging problem.

In order to facilitate the observation of NH_3^+ in astrophysical environments it would clearly be desirable to simulate the rotational spectra of NH_2D^+ and NHD_2^+. The computer program XY3 employed in the present work, however, only permits calculations for pyramidal molecules with $D_{3h}(M)$ [26,27] molecular symmetry group. We are currently extending the newly developed program

TROVE [57], which can treat NH_2D^+ and NHD_2^+, by modules to calculate rovibrational intensities. The simulation of the rotational spectra of NH_2D^+ and NHD_2^+ will be one of the first applications of the extended program and will be the subject of a future publication. Also, we plan further theoretical work on the Raman spectra of four-atomic pyramidal molecules. Recently, we have computed full-dimensional *ab initio* polarizability tensor surfaces for NH_3 and SbH_3, and these surfaces will be used for predicting Raman intensities.

Acknowledgements

Appendix A. Supplementary material

Supplementary data associated with this article can be found, in the online version, at doi:10.1016/j.chemphys.2008.01.052.

References

[1] M.G. Bawendi, B.D. Rehfuss, B.M. Dinelli, M. Okumura, T. Oka, J. Chem. Phys. 90 (1989) 5910.
[2] S.S. Lee, T. Oka, J. Chem. Phys. 94 (1991) 1698.
[3] T.R. Huet, Y. Kabbadj, C.M. Gabrys, T. Oka, J. Mol. Spectrosc. 163 (1994) 206.
[4] P.J. Miller, S.D. Colson, W.A. Chupka, Chem. Phys. Lett. 145 (1988) 183.
[5] W. Habenicht, G. Reiser, K. Müller-Dethlefs, J. Chem. Phys. 95 (1991) 4809.
[6] G. Reiser, W. Habenicht, K. Müller-Dethlefs, J. Chem. Phys. 98 (1993) 8462.
[7] M.R. Dobber, W.J. Buma, C.A. de Lange, J. Phys. Chem. 99 (1995) 1671.
[8] B. Niu, M.G. White, J. Chem. Phys. 104 (1996) 2136.
[9] H. Dickinson, D. Rolland, T.P. Softley, Philos. Trans. R. Soc. London, Ser. A 355 (1997) 1585.
[10] D. Edvardsson, P. Baltzer, L. Karlsson, B. Wannberg, D.M.P. Holland, D.A. Shaw, E.E. Rennie, J. Phys. B 32 (1999) 2583.
[11] H. Dickinson, D. Rolland, T.P. Softley, J. Phys. Chem. A 105 (2001) 5590.
[12] Y. Song, X.-M. Qian, K.-C. Lau, C.Y. Ng, J. Liu, W. Chen, J. Chem. Phys. 115 (2001) 2582.
[13] R. Seiler, U. Hollenstein, T.P. Softley, F. Merkt, J. Chem. Phys. 118 (2003) 10024.
[14] M.-K. Bahng, X. Xing, S.J. Baek, C.Y. Ng, J. Chem. Phys. 123 (2005) 084311.
[15] M.-K. Bahng, X. Xing, S.J. Baek, X. Qian, C.Y. Ng, J. Phys. Chem. A 110 (2006) 8488.

[16] W.E. Thompson, M.E. Jacox, J. Chem. Phys. 114 (2001) 4846.
[17] H. Ågren, I. Reineck, H. Veenhuizen, R. Maripuu, R. Arneberg, L. Karlsson, Mol. Phys. 45 (1982) 477.
[18] P. Botschwina, Habilitation Thesis, University of Kaiserslautern, 1984.
[19] P. Botschwina, J. Chem. Soc., Faraday Trans. 84 (1988) 1263.
[20] P. Botschwina, in: J.P. Maier (Ed.), Ion and Cluster Ion Spectroscopy and Structure, Elsevier, Amsterdam, 1989.
[21] W.P. Kraemer, V. Špirko, J. Mol. Spectrosc. 153 (1992) 276.
[22] W.P. Kraemer, V. Špirko, J. Mol. Spectrosc. 153 (1992) 285.
[23] P. Pracna, V. Špirko, W.P. Kraemer, J. Mol. Spectrosc. 158 (1993) 433.
[24] C. Woywod, S. Scharfe, R. Krawczyk, W. Domcke, H. Köppel, J. Chem. Phys. 124 (2006) 5880.
[25] A. Viel, W. Eisfeld, S. Neumann, W. Domcke, U. Manthe, J. Chem. Phys. 124 (2006) 214306.
[26] P.R. Bunker, P. Jensen, Molecular Symmetry and Spectroscopy, second ed., NRC Research Press, Ottawa, 1998.
[27] P.R. Bunker, P. Jensen, Fundamentals of Molecular Symmetry, IOP Publishing, Bristol, 2004.
[28] W. Meyer, J. Chem. Phys. 58 (1973) 1017.
[29] S.N. Yurchenko, M. Carvajal, P. Jensen, H. Lin, J.J. Zheng, W. Thiel, Mol. Phys. 103 (2005) 359.
[30] S.N. Yurchenko, M. Carvajal, W. Thiel, H. Lin, P. Jensen, Adv. Quant. Chem. 48 (2005) 209.
[31] H. Lin, W. Thiel, S.N. Yurchenko, M. Carvajal, P. Jensen, J. Chem. Phys. 117 (2002) 11265.
[32] S.N. Yurchenko, M. Carvajal, H. Lin, J.-J. Zheng, W. Thiel, P. Jensen, J. Chem. Phys. 122 (2005) 104317.
[33] S.N. Yurchenko, M. Carvajal, P. Jensen, F. Herregodts, T.R. Huet, Chem. Phys. 290 (2003) 59.
[34] S.N. Yurchenko, W. Thiel, S. Patchkovskii, P. Jensen, Phys. Chem. Chem. Phys. 7 (2005) 573.
[35] S.N. Yurchenko, M. Carvajal, W. Thiel, P. Jensen, J. Mol. Spectrosc. 239 (2006) 71.
[36] S.N. Yurchenko, W. Thiel, P. Jensen, J. Mol. Spectrosc. 240 (2006) 197.
[37] M.B. Bell, L.W. Avery, J.K.G. Watson, Astrophys. J. Suppl. 86 (1993) 211.
[38] A.T. Tokunaga, R.F. Knacke, S.T. Ridway, L. Wallace, Astrophys. J. 232 (1979) 603.
[39] S.S. Prasad, L.A. Capone, J. Geophys. Res. 81 (1976) 5596.
[40] H. Kawakita, K. Ayani, T. Kawabata, Publ. Astron. Soc. Japan 52 (2000) 925.
[41] H. Kawakita, J. Watanabe, D. Kinoshita, S. Abe, R. Furusho, H. Izumiura, K. Yanagisawa, S. Masuda, Publ. Astron. Soc. Japan 53 (2001) L5.
[42] H. Kawakita, J. Watanabe, S. Ando, W. Aoki, T. Fuse, S. Honda, H. Izumiura, T. Kajino, E. Kambe, S. Kawanomoto, K. Noguchi, K. Okita, K. Sadakane, B. Sato, M. Takada-Hidai, Y. Takeda, T. Usuda, E. Watanabe, M. Yoshida, Science 294 (2001) 1089.
[43] L.M. Ziurys, A.J. Apponi, J.T. Yoder, Astrophys. J. 397 (1992) L123.
[44] MOLPRO, version 2002.3 and 2002.6, a package of *ab initio* programs written by H.-J. Werner and P.J. Knowles, with contributions from R.D. Amos, A. Bernhardsson, A. Berning et al.
[45] C. Hampel, K. Peterson, H.-J. Werner, Chem. Phys. Lett. 190 (1992) 1, and references therein. The program to compute the perturbative triples corrections has been developed by M.J.O. Deegan, P.J. Knowles, Chem. Phys. Lett. 227 (1994) 321.
[46] G.D. Purvis, R.J. Bartlett, J. Chem. Phys. 76 (1982) 1910.
[47] M. Urban, J. Noga, S.J. Cole, R.J. Bartlett, J. Chem. Phys. 83 (1985) 4041.
[48] K. Raghavachari, G.W. Trucks, J.A. Pople, M. Head-Gordon, Chem. Phys. Lett. 157 (1989) 479.
[49] T.H. Dunning, J. Chem. Phys. 90 (1989) 1007.
[50] D.E. Woon, T.H. Dunning, J. Chem. Phys. 98 (1993) 1358.
[51] D.E. Woon, T.H. Dunning, J. Chem. Phys. 103 (1995) 4572.
[52] S.-G. He, J.-J. Zheng, S.-M. Hu, H. Lin, Y. Ding, X.-H. Wang, Q.-S. Zhu, J. Chem. Phys. 114 (2000) 7018.
[53] R. Marquardt, M. Quack, I. Thanopulos, D. Luckhaus, J. Chem. Phys. 119 (2003) 10724.
[54] D. Papoušek, M.R. Aliev, Molecular Vibrational–Rotational Spectra, Elsevier, Amsterdam, 1982.
[55] A.R. Edmonds, Angular Momentum in Quantum Mechanics, Princeton University Press, Princeton, 1974.
[56] G. Avila, J.M. Fernández, B. Maté, G. Tejeda, S. Montero, J. Mol. Spectrosc. 196 (1999) 77.
[57] S.N. Yurchenko, W. Thiel, P. Jensen, J. Mol. Spectrosc. 245 (2007) 126.